Analysis of non-coding functional elements of gene in zebrafish

and

Epigenetic studies in a human developmental disorder

By Amy Amelia Slater

15th August 2011

A thesis submitted to the University of Birmingham of the degree of MASTERS OF RESEARCH

This project is submitted in partial fulfillment of the requirements for the award of the MRes'

Clinical and Experimental Medicine
College of Medical and Dental Sciences,
University of Birmingham

Contents

List of abbreviations

ART: Assisted Reproductive Technologies

AS: Angelmans Syndrome

ATAC: Ada-two-A Containing HAT complex

BWS: Beckwith-Wiedemann Syndrome

CFP: Cyan Fluorescent Protein

CNV: Copy Number Variation

CTCF: CCCTC Binding Factor

dH2O: Distilled Water

DMR: Differentially Methylated Region

GNAS: *GNAS Complex Locus*

GOM: Gain Of Methylation

GRB10: *Growth Factor Receptor Binding Protein*

HAT: Histone Acetyltransferase

HM: Hyper Methylation

Hpf: Hours post fertlisation

IC: Imprinting Center

IGF2: *Insulin like Growth Factor 2*

IGF2R: *Insulin like Growth Factor Receptor 2*

IM: Intermediate methylation

LOM: Loss Of Methyaltion

mat: maternal

MBD: methyl-CpG binding proteins

Mo: Morpholino

msx: *Muscle Segment Homobox*

NGN: *Neurogenin*

oep: *One eyed Pinhead*

PEG3:*Paternally Expressed Gene 3*

PLAGL1: *Pleiomorphic Adenoma Gene 1*

PWS: Parda-Willi Syndrome

RFP: Red Fluorescent Protein

SAGA: Spa-Ada Gcn 5

SD: Standard deviation

SEM: Standerd Error Mean

Shh: *Sonic Hedgehog*

SNRPN: *Small Nuclear Ribnucleoprotein polypeptide N*

SRS: *Silver Russell Symdrome*

TNDM: Transient Neonatal Diabetes Mellitus

UM: Unmethylated

UPD: Uniparental Disomy

UTR: Untranslated Region

zzz3: *Zinc finger protein zz type 3*

Analysis of non-coding functional elements of gene in zebrafish

By

Amy Amelia Slater

A thesis submitted to the University of Birmingham of the degree of MASTERS OF RESEARCH

This project is submitted in partial fulfillment of the requirements for the award of the MRes'

Clinical and Experimental Medicine
College of Medical and Dental Sciences,
University of Birmingham

Abstract

Cis-regulatory regions such as enhancers are associated with regulating transcription of target genes. Many of these regulatory regions are distally located over 1kb away from their target promoter, and many studies been conducted to identify how enhancer and promoter regions are brought into proximity to allow interaction and initiation of transcription. Such research has identified protein complexes such as SAGA and ATCA, which bind to specific enhancers and promoters bringing them into close proximity. This study focuses on one unique subunit of the ATAC complex, zzz3. By knocking down expression of zzz3 in zebrafish by morpholino injection, the role *zzz3* plays in development and phenotype can be determined. It was observed during this study that *zzz3* knockdown resulted in a bent tail and ventralisation of embryos, suggesting a potential role for this protein in the development of the floor plate and notochord.

Introduction

Cis regulator regions

Initiation of gene transcription is a complex system involving rearrangement of chromatin into a permissive state by histone modifications. This is followed by the recruitment of many transcription factors, and co-activators to a gene's promoter region before transcription via RNA polymerase II can occur. Transcription is often regulated by *cis*-regulatory regions located in non-coding regions of the DNA, including enhancers (associated with increased gene transcription) and insulators (protecting genes from transcription), located either within 1Kb (proximal promoter elements) or >1Kb (distal elements) of the transcription start site (Krebs, A Thesis 2010; Epstein. D 2009).

Mutations within the *cis*- regulatory regions of the human genome have been attributed to 1-2% of disease causing mutations and are responsible for conditions such as preaxial polydactyly, where a mutation in the upstream *Sonic hedgehog (Shh*) enhancer results in extra digits forming during development. A mutation in the *IRF6* enhancer results in an increased risk of non-syndromes cleft palate (Epstein.D 2009).

Zebrafish

Zebrafish (*Danio rerio*) are an established model organism for the study of human disease and embryonic development, becoming popular due to its ease of use, relatively low maintenance costs, ability to produce large quantities of embryos each mating, permitting semi high throughput screening assays (either

pharmaceutical or genetic). Embryos are transparent and develop rapidly outside of the mother, removing the need to dispatch the mother (Fleming.A 2007). Zebrafish have therefore been used in many studies and even as a model for studied in to the genetic basis for human diseases such as muscular dystrophy (Kawahara.G et al 2010). Other groups have been investigating the genetics employed by zebrafish in heart regeneration after damage, to better understand mechanisms that could potentially be translated into treating human heart disease (Jopling et al 2010).

Zebrafish have also proved indispensable in the search for enhancers and other cis-regulatory regions. For example Müller.F et al 1999, successfully mapped the *shh* enhancer location and identified that the enhancer is split into 3 regions across two introns, as well as identifying in which tissues each enhancer region promotes *shh* expression, such as the notocord, and the floorplate. The identification of enhancer regions presents many challenges, predominantly due the promiscuity of enhancer interactions. Therefore, to aid discovery, screens of enhancer promoter constructs have been conducted. Zebrafish provide an excellent model for in vivo analysis for these constructs. With the advances in technology it has now become possible to map these construct in zebrafish in a high throughput manner (Gehrig.J et al 2009).

Zebrafish are an essential model organism of developmental genetics and more recently emerged as models for human disease. Coupled with advances in technology, such as development of high throughput assays and specific gene knock down by morpholino oligonucleotides, the zebrafish provides a basis for many more genetic, developmental investigations.

Morpholino (Mo) technology

A key development in targeted gene knockdown in vivo was the development of Mo, chemically altered oligonucleotides with high affinity for mRNA. These inhibit mRNA translation in an RNaseH endonucleoase independent manner (Nasevicius. A & Stephen .C 2000) via blocking the progression of the ribosome along the mRNA, in a similar mechanism to RNAi technology, or preventing proper mRNA splicing (Eisen and Smith 2008; Bill. BR et al 2008). Mo's are chemically modified bases consisting of a six membered morpholino ring, instead of the standard ribose ring found in RNA, linked together to form oligonucleotides. This modification increases the stability of the oligonucleotides, and renders them resistant to nucleases. Another key feature of Mo oligonucleotides is that they do not possess a negatively charged backbone, unlike RNA and DNA. This means that nonspecific interactions are reduced and therefore Mo is likely to be less toxic to cells than RNAi (Eisen and Smith 2008).

When designing Mo oligonucleotides, it is advised that the Mo is a maximum of around 25 bases long with no secondary structure, designed to be complementary for the target mRNA transcript. To ensure the effects observed after Mo injection are true findings it is widely advisable to design at least two Mo's for different regions of the gene under investigation, for example the transcription start site (ATG Mo) and a 5' Untranslated region (UTR Mo) (both are designed to inhibit translation) or a Mo targeted to an intron of pre spliced mRNA (splice Mo), preventing proper splicing, thus removing the functional protein. Splice Mo's; however do not affect the maternally inherited mRNA, which is already spliced. A miss match control (with at least 5 bases different from functional Mo) should also

be included in experiments to control for potential off target effects. (Eisen and Smith 2008; Bill.BR et al 2008).

This technique of gene knockdown has been demonstrated as an effective technique for use in zebrafish. Initial studies using this technique knocked down previously well characterised genes such as *one-eyed pinhead gene (oep), Shh* and *nacre* to determine the usefulness and reliability of Mo technology in zebrafish (Nasevicius.A & Stephen C. 2000). Since the initial studies Mo injections have become a widely accepted technique for gene knockdown within zebrafish models, and have since been involved in many studies of gene function, such as identifying the role of *muscle segment homebox* genes *msxB, C and E* play a role in neural crest development (Pillips. BT et al 2006).

Ada-Two-A Containing (ATAC) histone acetyltransferase complex

The ATAC histone acetyltransferase (HAT) complex was identified in Drosophila in 2008; since then it has been demonstrated that this HAT complex binds to both enhancers and promoters, bringing the two into proximity thus aiding transcription (Krebs.A Thesis 2010; Nolis.IK et al 2009).

ATAC has been reported to consist of several proteins, including the acetyltransferase GCN5 or PCAF (only one type per complex). GCN5 acetylates H3K9 (Histone 3 Lysine 9) and H3K14 (histone modifications permissive of transcription) and in combination with adaptor proteins ADA2-A (required to maintain GCN5 association with the ATAC complex) and ADA3 forms the catalytic core of ATAC (Orpinell.M et al 2010). Other proteins associated with the complex include nucleosome remodelling proteins (E.g Wdr5), MAP kinase regulator

(MBIP), the stress and TGFβ activated protein kinase (TAK1). As well as a NC2β histone fold protein that was identified to interact with TATA binding protein and inhibit transcription (Wang. YL et al 2008), and zzz3 (zinc finger protein ZZ type 3) a potential DNA binding protein unique to ATAC, (Krebs.A Thesis 2010) other proteins are also involved in this complex but are not mentioned in this report. This huge diversity of proteins involved in the ATAC complex highlights the intricacy of the potential functions with which ATAC may be associated.

ATAC was initially identified as structurally similar but functionally different to the SAGA (Spa ada Gcn5) complex. However closer analysis has determined that both complexes share some subunits such as GCN5 and Ada3, while others such as zzz3 are unique to ATAC (Krebs.A Thesis 2010). The same group (Krebs. AR et al 2011) also identified that SAGA is preferentially found at promoters, while ATAC was identified to bind both promoters and a distinct novel class of cell and gene specific enhancers that do not bind the common transcriptional co-activators p300.

Studies into the function of ATAC have identified an association with non-histone proteins, and cellular functions such as mitosis. The GCN5 subunit in ATAC was shown to acetylate cyclin A thereby altering its stability, thus regulating downstream mitotic progression. While knockdown of ATAC results in delayed M/G1 transition (Orpinell,M et al 2010), Suganuma.T et al 2010 identified an alternative function of ATAC in Drosophila in the regulation of JNK target genes and p53 when under osmoitic stress, via the MAP kinase subunit. They concluded that ATAC was vital for maintaining a balance between the JNK induced proliferation and p53 mediated cell death.

Although investigation into the role of ATAC and the relevant subunits is being undertaken, there is so far no investigation into the in vivo function of the *zzz3* subunit.

As mentioned, *zzz3* is a unique subunit of ATAC, however its function within this complex is as yet unknown. It is hypothesised that *zzz3* plays a role in the binding of ATAC to its specific enhancers (Krebs.A Thesis 2010). This study therefore intends to investigate via reverse genetic techniques the role of *zzz3* in zebrafish development by analysing knock-down phenotypes.

Methods and Materials

Fish Care

Initial investigation of *zzz3* was performed on wild type Danio rerio AB*, further investigation into the effects of *zzz3* on neuronal development was preformed on a stable transgenic line *Neurogenin- rfp (NGN-rfp).* All fish were cared for according to the standard protocols (Westerfield, M 1995). Fish were maintained in mixed sex tanks at 28°C, on a 12 hour light and dark cycle, and fed twice daily.

Collection of embryos

The night before egg collection (post feeding), breeding cages complete with inlays and dividers were filled with water. Fish from desired tanks were paired up male and female, with no more than 4 fish per cage and the dividers preventing males and females interacting. Fish were left undisturbed over night.

The following morning, water in the breeding cages was replaced to aid cleaning of embryos, dividers were removed and fish left for approximately 10 minutes to breed. The cage inlays allowed for the eggs to fall to the bottom of the cage and protect them from being consumed by the adult fish. Once the eggs were laid, the inlay and the adult fish were transferred to a fresh cage of water, while the water in cage containing the embryos was poured through a fish net trapping the embryos which were in turn transferred to a 5ml Petri dish with a small amount of fish water. This process of embryo collection was repeated for all fish pairs that had laid. Floating debris was carefully poured off, and the embryos were pipetted into separate 5ml Petri dishes (one dish per injection solution) with approximately 100 embryos per plate. Embryos were swirled to reside in the

centre of the dish before all water was removed using a fine plastic pipette. Surface tension ensures the embryos are held stationary during injections.

Injections

Injection solutions containing *zzz3* Morpholinos (Mo) (Gene tools LLC) either specific for ATG start site, 5' UTR, or a 5 base mismatch control (sequence found in Table 1) were created to a concentration of 100μM or 200μM in a final volume of 10μl. Included in the injection solutions was 5% rhodamine dextran (Invitrogen) (required for sorting successfully injected embryos), 0.5% phenol red (Sigma) (required to visualise the amount of injection and which embryos are injected) and nuclease- free water. It should be noted that Rhodamine and *Red Fluoresce protein (rfp)* both fluoresce at similar wavelengths, therefore when creating the injection solution for the *NGN- rfp* transgenic embryos, Rhodamine was substituted with *CFP-mRNA* at a concentration of 15ng/μl.

Table 1: Morpholino sequence

Morpholino	**Sequence**
Mismatched Control	CATcGTGgTCTCTgCTCAcCAGgAG
ATG	CATGGTGCTCTCTCCTCAGCAGCAG
5' UTR	AGCTTGAACCATCCCATAGCAGTG

Morpholinos were stored at -20° C to reduce the risk of evaporation, however this leaves the stock solutions prone to precipitation, therefore it was vital that before any use, the morpholinos were heated at 65°C for 5 min. The homology of each Mo sequence was also determined via BLAST analysis against the zebrafish genome Zv9 (UCSC).

Injection needles were created from 2mm diameter capillary tubing using a heat filament needle puller to crate a fine tip. Needles were loaded with approximately 2µl injection solution ensuring that no air bubbles were present, before being inserted in to a brass needle holder attached to a pressurised nitrogen cylinder. The nitrogen gas pressure was adjusted to 200psi though this was often changed depending on the size of the needle hole to ensure equal amount of injection solution was dispensed for each morpholino.

Using a fine tipped forceps the top 1/3 of the needle tip was removed. To test that the needle hole was not too large or the air pressure too high some injection solution was ejected and the volume dispelled was visually assessed. It was important to keep the droplet size consistent between injection solutions and experiments.

Under a light microscope, the injection needle was gently inserted through the chorion and into the yolk/ single cell (embryos that have developed past the single cell stage were not injected), using a foot pedal dispelled injection solution. If correctly administered the diameter of the injection solution should reach1/10th of the embryo diameter, which was determined by eye (Fig 1A).

A.

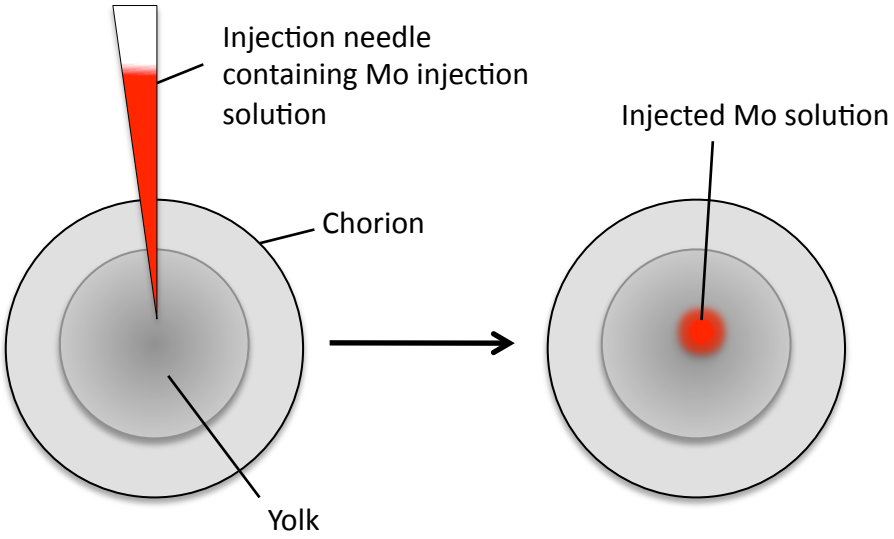

B.

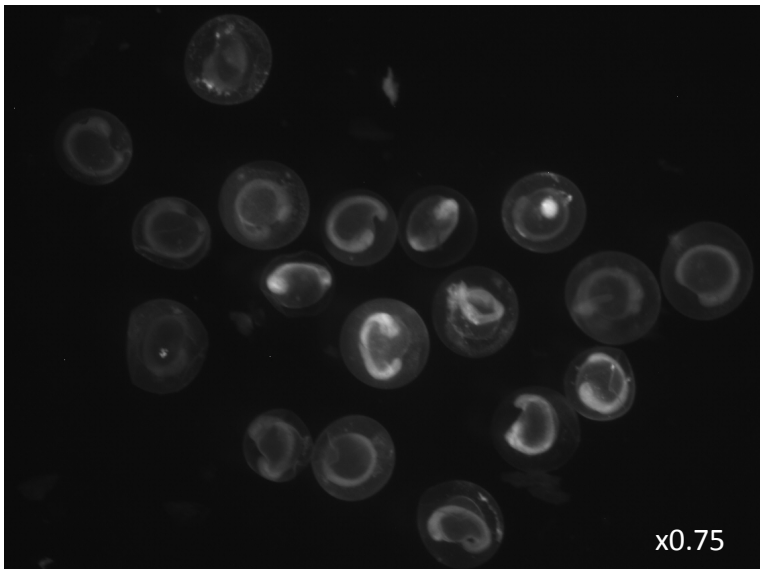

FIG 1: Injection of single cell embryos. A) Diagrammatic representation of microinjection of single cell embryos. Injection solution (red) should occupy 1/10th of the embryo. B) Rhodamine sorting of injected embryos at 20hpf. Non- injected embryos not visible under fluorescent microscope.

Post injection care

Embryos were maintained at 28°C in an incubator, the optimal temperature for development. Following injection, embryos were re-suspended in 1x E3 medium (5 mM NaCl, 0.17 mM KCl 0.33 mM $CaCl_2$, 0.33 mM $MgSO_4$) with Gentamicin sulfate ((Fish Bioreagents) 0/5ml in 1litre 1x E3) to prevent fungal or bacterial infection. After injections embryos were left to recover briefly prior to being cleaned. A plastic pipette was used to remove and discard all dead and non-fertilised eggs. Living embryos were transferred to a 10ml Petri dish and fresh E3 Gent media was added. The media was changed every 24 hours and the dead removed to avoid paramecium infection.

Sorting

Injected embryos were sorted from non-injected embryos by using the fluorescent marker (rhodamine or cfp-mRNA) incorporated in the injection solution, and viewed under a fluorescent microscope (Nikon). For embryos injected with rhodamine this was usually done between 4-20 hpf (Fig 1B). With *CFP*-mRNA this sorting step could not be completed until *CFP*-mRNA was translated into a large enough quantity to be visulised so was usually undertaken at around 20hpf.

Dechorionation

In order to clearly visualise phenotypes in developing embryos, it was necessary to remove embryos from their chorion. For this project embryos were dechorionated at 24hpf enzymatically by Pronase type XIV (Sigma – Aldrich). The full protocol is found at Chen Lab protocols Stanford University.

In summery, most media was removed from the embryos, and 1ml of pronase in de-ionised water (10mg/ml) was added to the embryos, and left for around 5 minutes. Occasional swirling helped to disrupt the chorion and aid the dechorionation. When approximately 1/3 of embryos were hatched, the plate was submersed in 1 liter of warmed fish water (2/3 deionised water 1/3 Normal) to dilute the pronase. Water was carefully tipped off and replaced. This was repeated 3 times, embryos were gently pipette up and down 3 times with a plastic pipetted to ensure all chorions were removed, before being transferred in to a fresh 10ml Petri dish with fresh E3 gent media.

Imaging

Embryos were imaged at 24 and 48hpf, using a Nikon fluorescent microscope with imaging software NSI elements.

In order to obtain a clear lateral view of the embryos a 3% agarose plate with furrows was made to hold embryos in the correct orientation. Mesab (0.03% in 1x E3 (Ethyl-3-aminobenzoate methansulfonate Sigma)) was added to sedate embryos allowing easy manipulation with forceps prior to imaging. To image, embryos were sorted in to groups of similar phenotypes and were photographed using software NIS elements. Images were captured with bright field and for *NGN-rfp* transgenic fluorescent imaging. Identification of neurons in *NGN-rfp* transgenic embryos was carried out by high magnification bright field and fluorescent imaging of the embryo trunk 24hpf and 48hpf. Neurogenin positive cells within 5 somites length above the yolk extension end were counted and documented for each treatment group.

Data Analysis

The fluorescence signal data was analysed using GraphPad Prism software. All data is presented as mean ± SEM, and statistical tests included Students t-test.

Results

Bioinformatic analysis of *zzz3* Mo

As the Mo were predesigned, bioinformatic analysis was conducted to confirm the location and homology of each Mo to the *zzz3* gene (Chromosome 2: 8563505-8625237:1), and to also determine if there was any off target homology that could be responsible for any phenotypes observed. The *zzz3* five base mismatch control Mo presented with 0% homology to the *zzz3*, confirming it to be a suitable control. The 5' UTR *zzz3* Mo was proven to be 100% homologous to the 5' UTR region of *zzz3* at Ch2: 8564791 – 8564814. While the start site Mo ATG *zzz3* showed a 96% homology, with one base difference to *zzz3* at location Ch2: 8564791 – 8564814, however this is still a high homology and the alternative base should not significantly effect the efficiency of the ATG Mo. No Mo used in this study showed homology to any other region of the zebrafish genome.

Phenotype analysis

Mo injections of either *zzz3* ATG Mo, zzz3 5' UTR Mo or *zzz3* mis-matched control Mo, were injected in to AB* wild type zebra fish embryos at single cell stage. Post cleaning and sorting, embryos were incubated until viewing for phenotypes during the pharyngula stage of development at 24 hpf (prim 5 stage) and 48 hpf (long pec stage (prim 11)) (Kimmel. C.B et al 1995).

A total of 1726 embryos ((100μM control n= 274, ATG n= 389 and UTR n= 275) (200 μM control n= 289, ATG n= 247 and UTR n= 252)) were observed for phenotypic abnormalities potentially caused by the *zzz3* Mo. Observed phenotypes were classified into four classes allowing the grouping of embryos with similar features to aid statistical comparison. **Class 1:** (Fig 2A for 24hpf Fig

3A for 48hpf) embryos present with wild type features consistent with the observations reported by Kimmel.CB et al 1995, during a study mapping the stages of zebrafish embryonic growth. **Class 2;** (Fig 2B for 24hpf Fig 3B for 48hpf) embryos have mild phenotype including slight pericardial oedama and slightly reduced head and eye size. A small amount of cell death my be observed in the head at 24 hpf, but trunk is similar to wild type. **Class 3;** (Fig 2C for 24hpf Fig 3C for 48hpf) embryos present with an increased severity of phenotype. The main feature visible was ventral tail (trunk) curvature, reduced yolk extension and mild ventralisation. Cell death observed in the head at 24hpf leading to decreased head and eye size, increased pericardial oedema, enlarged heart (visible at 48hpf) and U shaped somites were other features also observed. **Class 4;** (Fig 2D for 24hpf Fig 3D for 48hpf) Most severe phenotype. Complete ventralisation, with very small/ no head. Almost no yolk extension enlarged heart, pericardial oedema, sluggish circulation and deformed somites.

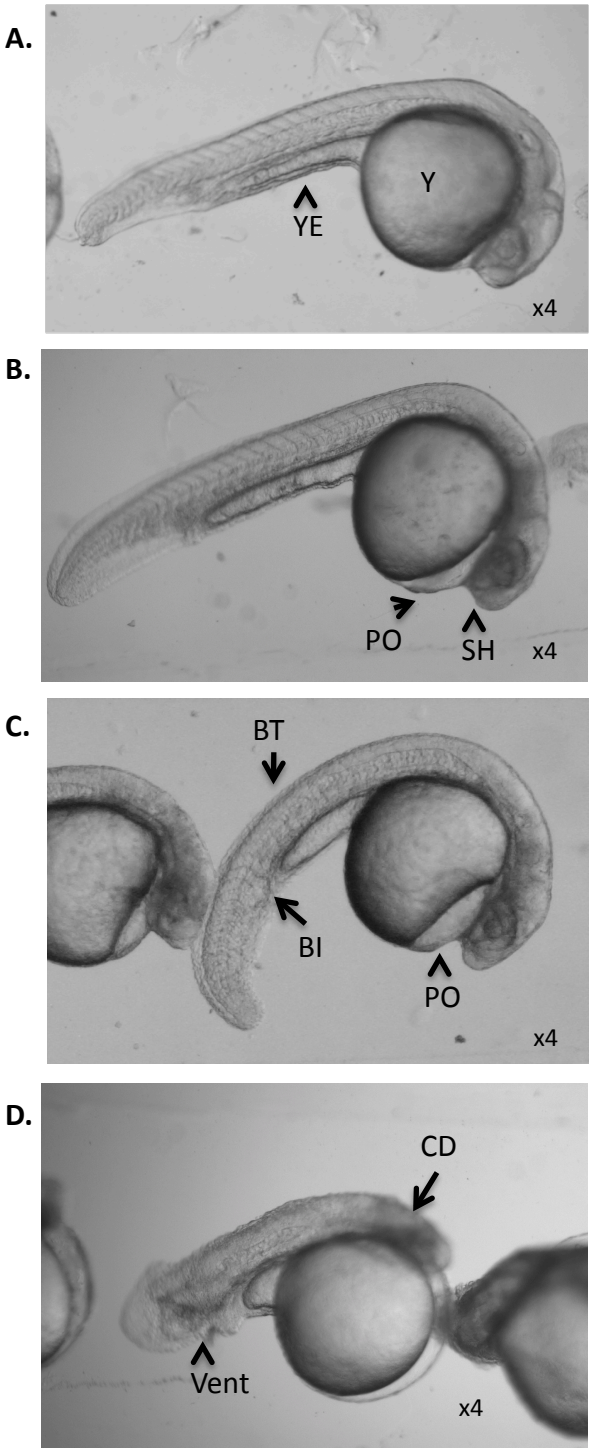

Fig 2: Bright field images of 24hpf embryos phenotype injected with *zzz3* Mo. Y= Yolk; YE=Yolk Extension; SH= Small head; PO= Pericardial oedema,; BT= Bent Tail; BI= Blood Island; CD= cell death; Vent= ventralisation including blood island. A) Class 1, wild type embryo. B) Class 2 phenotype embryo, slight decreased head size and pericardial oedema. C) Class 3 phenotype embryo, Bent tail, small head, blood island and pericardial oedema. D) Class 4 phenotype embryos; complete ventralisation of embryos, cell death in head visible and pericardial oedema.

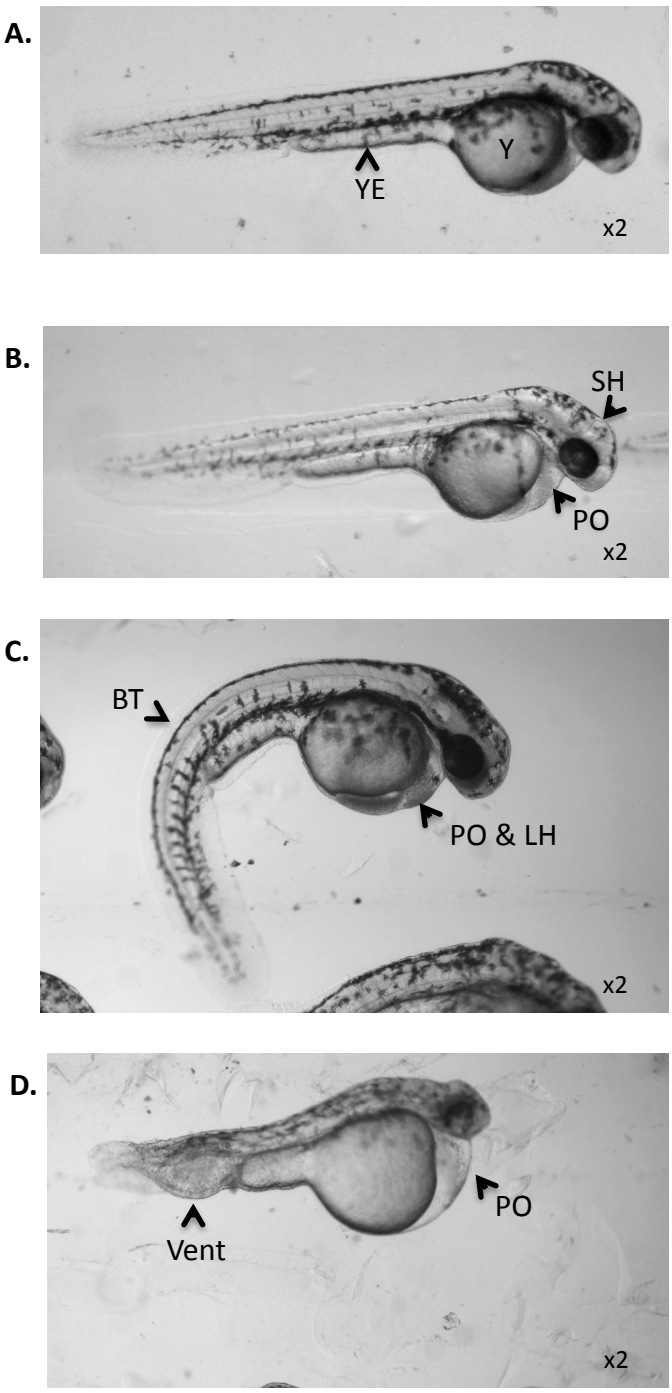

Fig 3: Bright field images of 48hpf embryos phenotype injected with *zzz3* Mo. Y= Yolk; YE=Yolk Extension; SH= Small head; PO= Pericardial oedema,; LH= enlarged heart BT= Bent Tail; Vent= ventralisation including blood island. A) Class 1, wild type embryo. B) Class 2 phenotype embryo, slight decreased head size and pericardial oedema. C) Class 3 phenotype embryo, Bent tail, small head, enlarged heart and pericardial oedema. D) Class 4 phenotype embryos; ventralised embryo, cell death caused small head and pericardial oedema.

The more severe the phenotype the less frequently it was observed, however every phenotype class was reported for every injection group. However, the frequency of embryos presenting with either a class 3 or class 4 phenotype was greater in those injected with *zzz3* ATG Mo, while a class 2 phenotype was more frequently observed in embryos injected with *zzz3* UTR morpholino.

At 24hpf, (Fig 4A and B) the percentage of ATG injected embryos presenting with a class 1 wild type phenotype was significantly lower than the frequency observed within the control group. With the higher ATG Mo concentration presenting the most significant reduction in class 1 phenotype compared to the control group (100μM ATG Mo P= 0.0106; 200μM ATG Mo P= 0.003). It should also be noted; that frequency of class 3 phenotype embryos at 24hpf was significantly increased in 200 μM ATG Mo embryos compared to the control group (P= 0.0008), however, there was also an increases in the frequency of control embryos presenting with either a class 3 or 4 phenotype when injected with the higher concentration Mo, suggesting potential non specific effects of the Mo. This trend was also observed within the 100μM ATG Mo, however, though it was not statistically significant. When evaluating the effects of the UTR Mo, it is interesting to note that apart from phenotype class 2 in the 200μM injection series, the prevalence of each phenotype class is very similar if not lower than the controls.

When directly comparing 100μM injection series to the 200μM injections, it was identified that for ATG Mo injections, the prevalence of class 3 phenotype was significantly more frequent in the 200μm population (P=0.0006), while the prevalence of wild type phenotype (class 1) was significantly more common in the 100μM injected embryos (P=0.019).

Most observations were also present at 48hpf, (Fig 5A and B) with the trend that ATG Mo increases the prevalence of the more severe phenotypes, in particular class 3 remaining consistent. However, due to handling error resulting in death, statistical analysis yielded less significant variation between injection groups than at 24hpf. It should also be noted that direct comparison between the two concentrations at this time point also revealed no significant difference in phenotype frequency.

Though many embryos presented with a wild type phenotype after *zzz3* knockdown, it should be noted that a tend was identified, where blockage of the *zzz3* transcript start site by the ATG Mo, resulted in an increased frequency of structural and developmental defects and ventralisation.

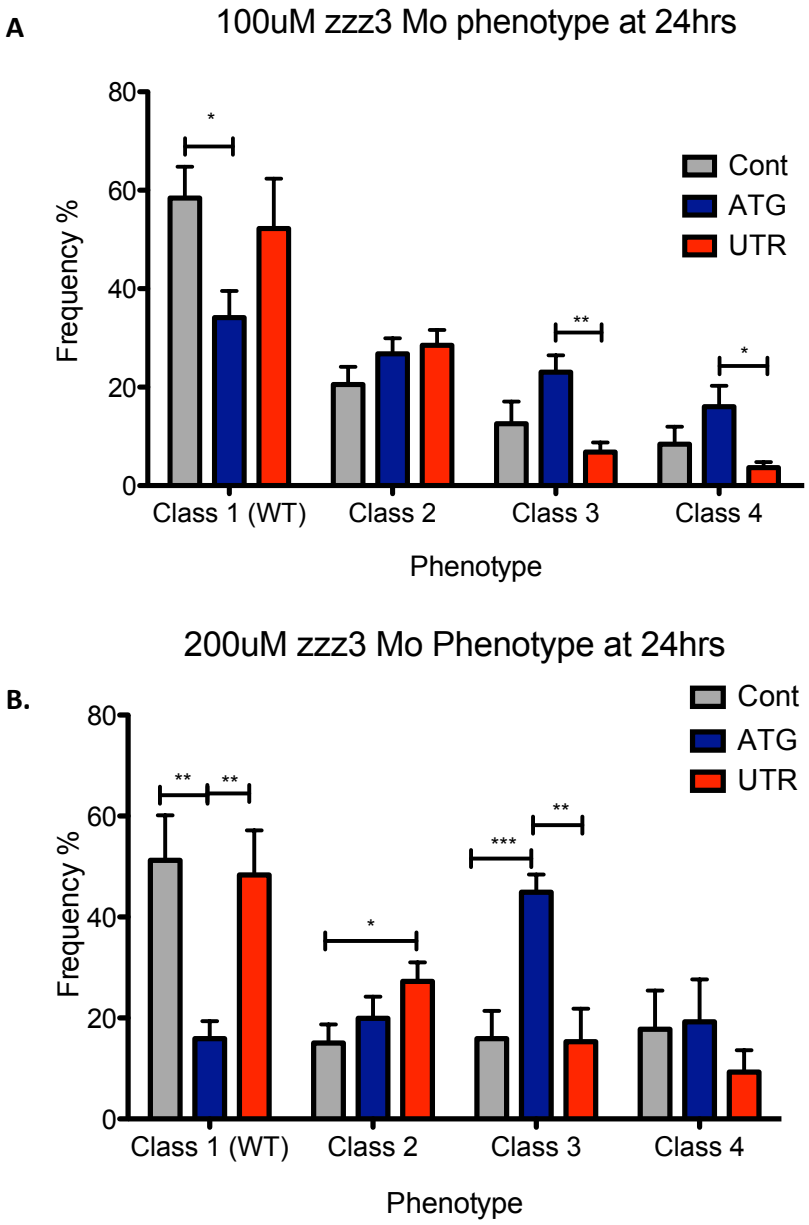

Fig 4: Frequency of embryos presenting with each phenotype class at 24hpf A) 100µM *zzz3* Mo injections, ATG Mo induces the frequency of embryos to present with a more severe phenotype. B) 200µM *zzz3* Mo injection, the effects of ATG are much more significant, but increase in control embryos presenting with severe phenotype suggests lack of specificity. Presented as mean± SEM. student t-test applied *=<0.05 **=<0.01 ***=<0.001

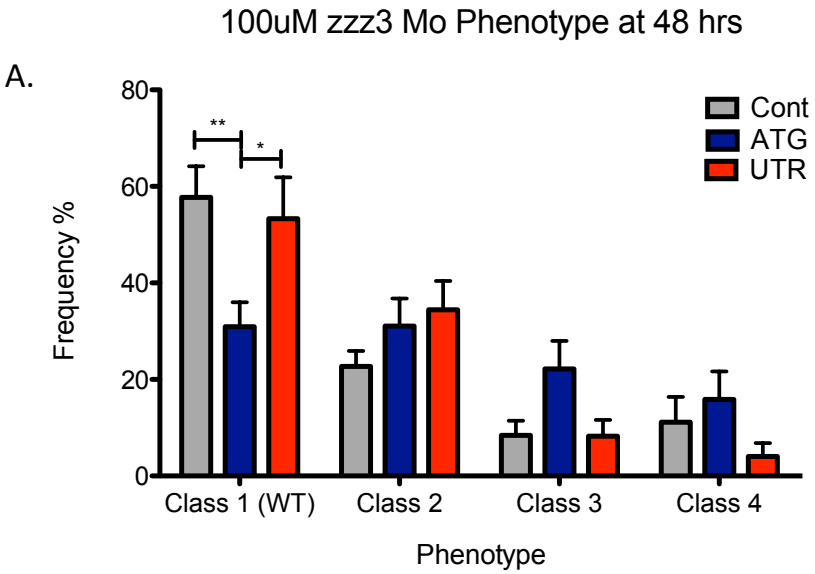

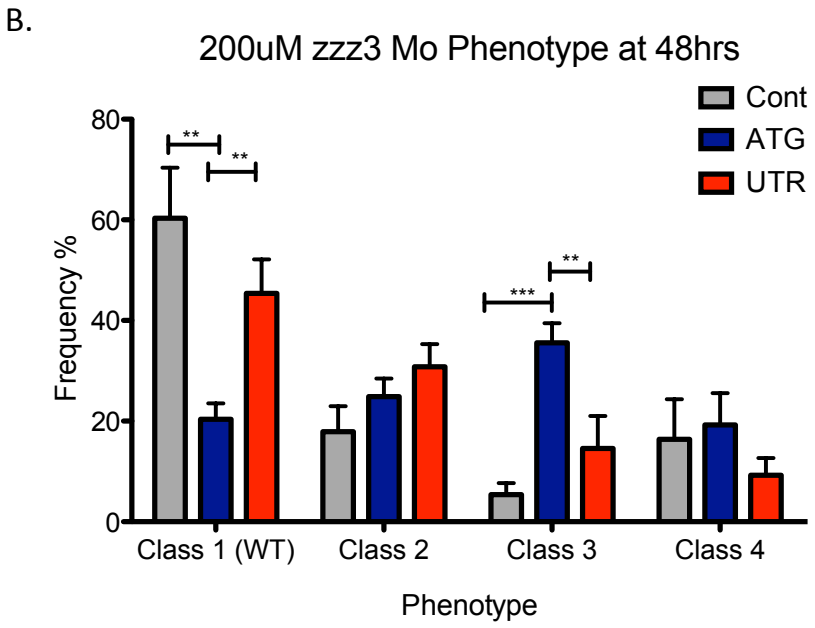

Fig 5: Frequency of embryos presenting with each phenotype class at 48hpf A) 100µM *zzz3* Mo injections, ATG Mo induces the frequency of embryos to present with a more severe phenotype. B) 200µM *zzz3* Mo injection, the effects of ATG are much more significant, but increase in control embryos presenting with severe phenotype suggests lack of specificity. Presented as mean± SEM. student t-test applied *=<0.05 **=<0.01 ***=<0.001

Zzz3 effect on neuronal development

A preliminary study was conducted upon transgenic embryos, expressing *neurogen–rfp (NGN-rfp)*. *NGN* is a transcription factor, found in many nerve cells within the zebrafish including the dorsal root ganglia, central nervous, neuronal crest and neuronal tube to name but a few, vital for the formation of peripheral sensory neurons (Zfin.org *neurogenin 1;* McGraw HF et al 2008,). It was therefore hypothesised that the curved phenotypes observed were due to midline defects such as loss of floor plate, which often lead to neural patterning defects. The *NGN-rfp* transgenic line was utilised in order to visualise the effect the *zzz3* Mo's may have on neuronal development, with potential events such as a reduction in neurons, may be observed in embryos with the curved phenotype. Embryos were injected with Mo at the single cell stage, and then imaged at 24(Fig 6A-D) and 48hpf (Fig 7A-D). High magnification photos of the trunk at the end of the yolk extension were captured in both bright field and under fluorescence. Images were then overlaid and numbers of fluorescent neurons in the neuronal tube within 5 somites of the end of the yolk extension documented. As this was a preliminary study only 75 transgenic embryos were investigated, therefore there were not always enough embryos of each phenotypes to obtain a SEM value or apply statistical analysis. In order to increase the number of embryos recorded per phenotype, phenotype class 1 and class 2 were pooled. Although no conclusions can be drawn from the data obtained, there is a suggestion that the more severe phenotypes Class 3 and Class 4 present with a lower number of neurons in the neuronal tube (24 hpf Fig 8A-B. 48hpf Fig 9A and B).

A.

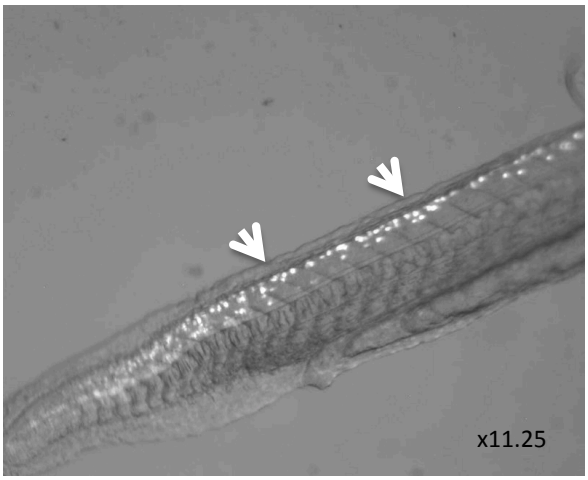

B.

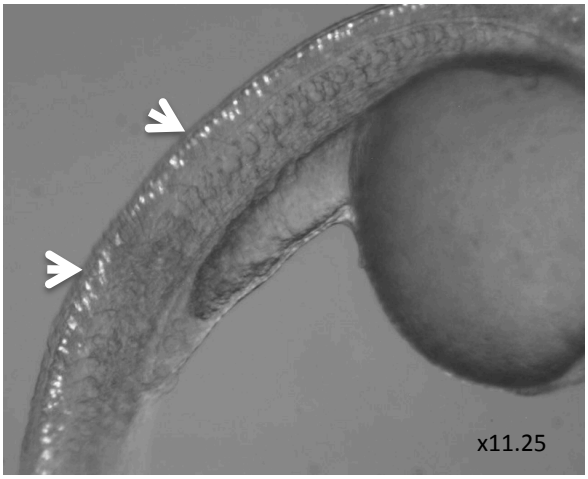

C.

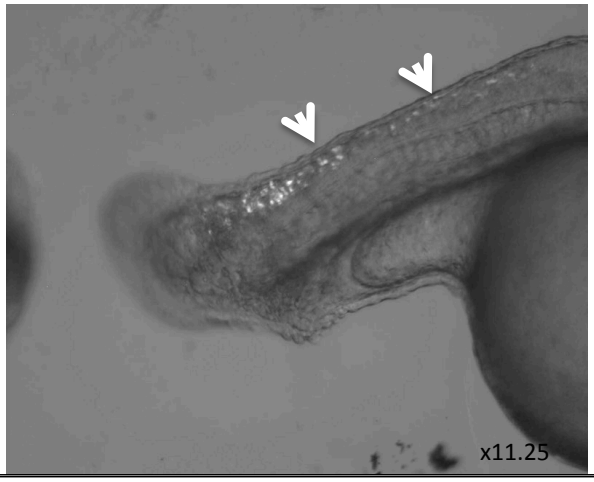

Fig 6: Overlay fluorescence and bright field images of the trunk of *NGN-rfp* transgenic embryos at 24hpf. A) Class 1 and 2 embryos, wild type or very mild phenotype. B) Class 3 phenotype embryos; bent tails. C) Class 4 phenotype embryos, presenting with ventralisation. white spots indicate neurogenin positive nerves, white arrows indicate the 5 somite region at the end of the yolk extention in which neurogenin nerves were counted.

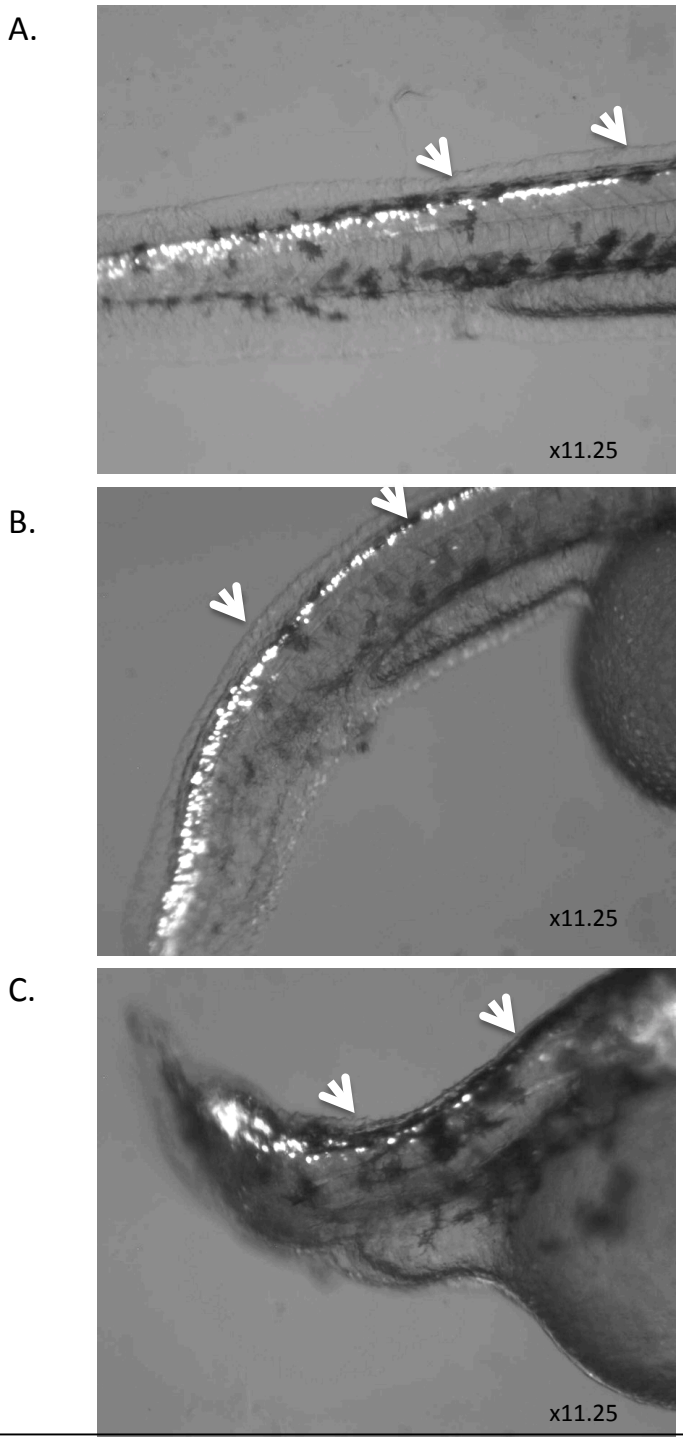

Fig 7: Overlay fluorescence and bright field images of the trunk of *NGN-rfp* transgenic embryos at 48hpf. A) Class 1 and 2 embryos, wild type or very mild phenotype. B) Class 3 phenotype embryos; bent tails. C) Class 4 phenotype embryos, presenting with ventralisation. White spots indicate neurogenin positive nerves, between white arrows indicates the 5 somite region in which neurogenin nerves were counted

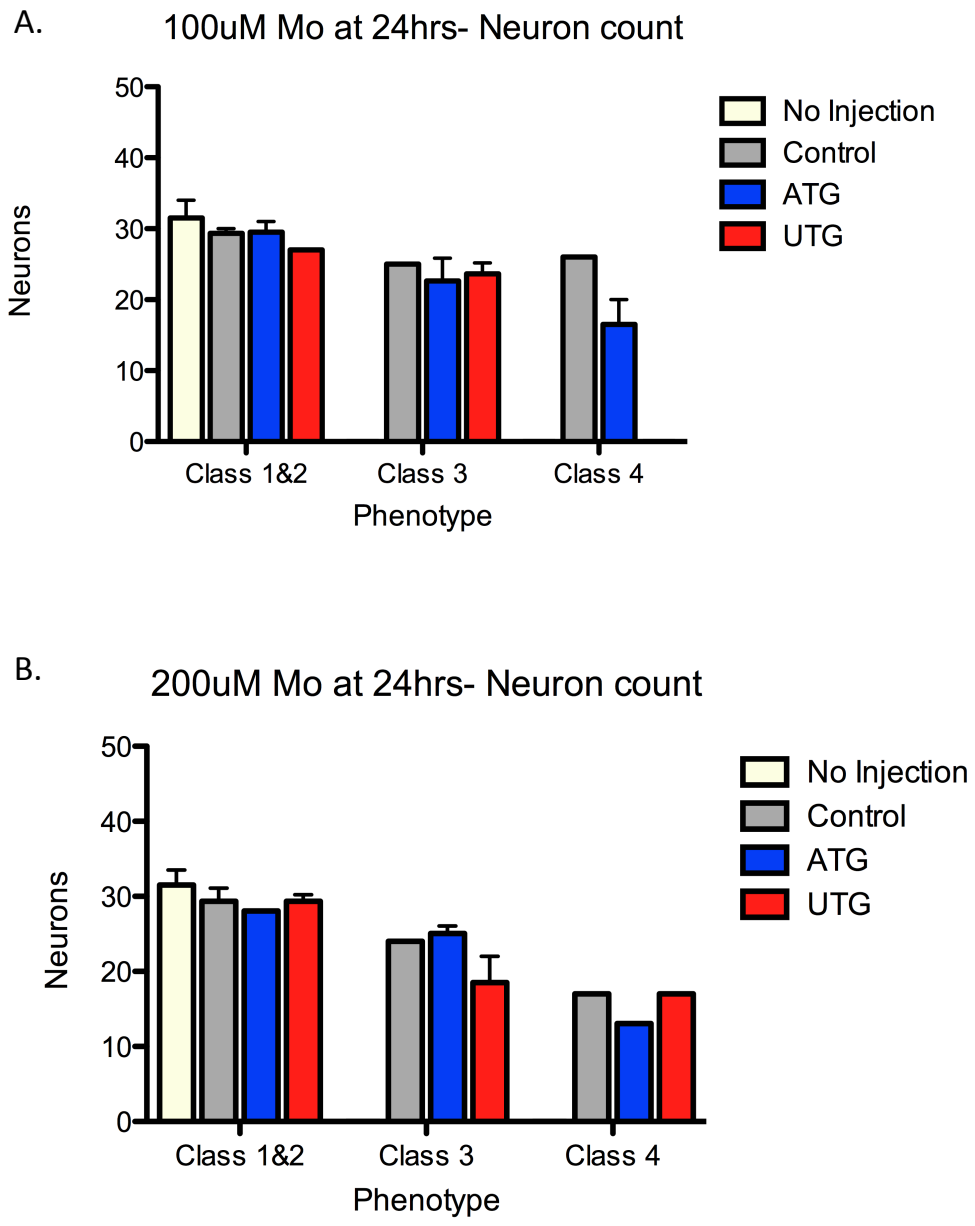

Fig 8: Frequency of neurogenin positive nerves in a five somite region previously indicated at 24hpf identifying a potential association between the number of peripheral neurons and the severity of the phenotype

A) 100µM *zzz3* Mo injections, B) 200µM *zzz3* Mo injection. Presented as mean± SEM where possible.

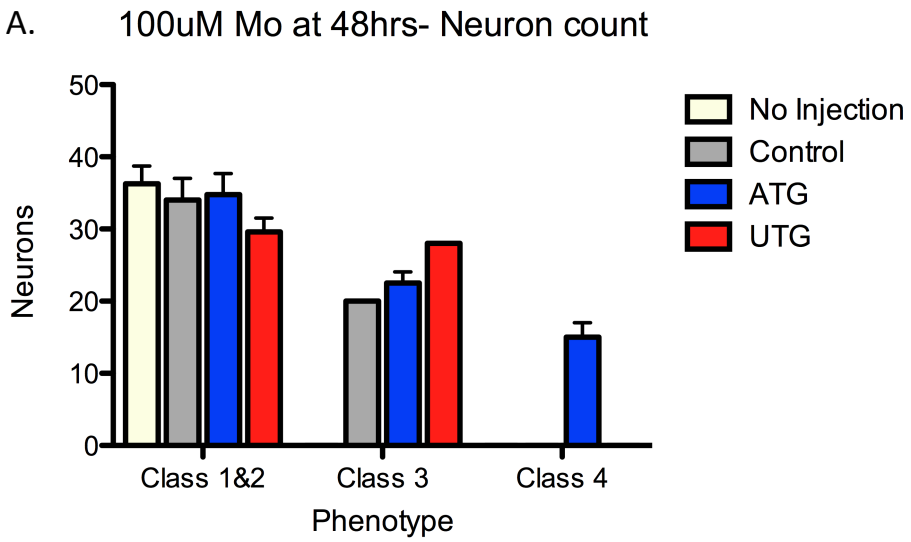

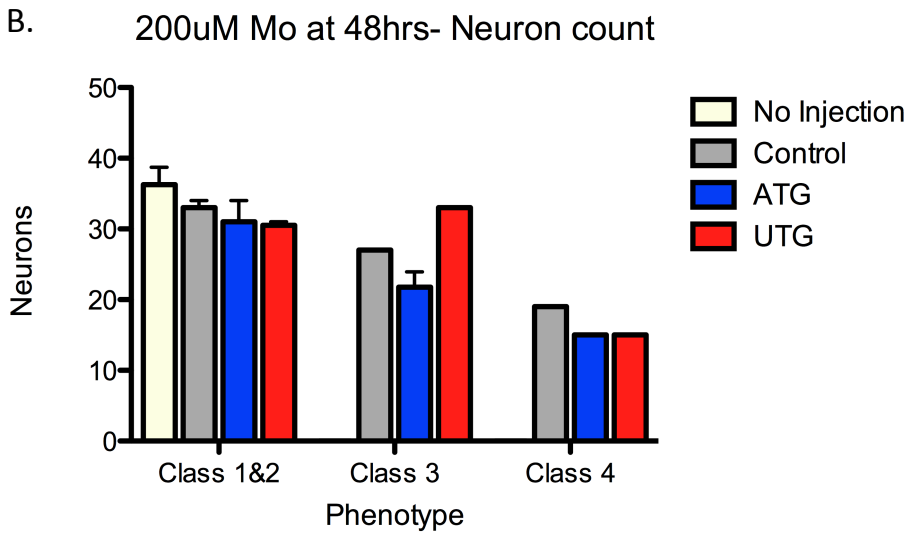

Fig 9: Frequency of neurogenin positive nerves in a five somite region previously indicated at 24hpf identifying a potential association between the number of peripheral neurons and the severity of the phenotype

A) 100µM *zzz3* Mo injections, B) 200µM *zzz3* Mo injection. Presented as mean± SEM where possible

Discussion

This initial study employed reverse genetics to identify and clarify the role of the ATAC subunit zzz3 upon zebrafish embryo phenotype. Knockdown of *zzz3* resulted in tail curvature, and general ventralisation of the embryos. This phenotype was more prevalent when knockdown was targeted to the TSS, with 100µM ATG Mo appearing to be the most specific concentration. Although 200µM Mo concentration also produced similar phenotypes, this was likely to be off target effects. The preliminary investigation conducted upon transgenic *NGN-rfp* indicated a potential loss of neuronal patterning, which if true, would be consistent with the hypothesis that the curved phenotypes observed was to be due to midline defects such as loss of floor plate or notochord, although it should be noted that no loss of notochord was visualised in this investigation. However, further investigation of neuronal patterning is required before any conclusions can be drawn.

Interestingly ATAC has been implicated to be involved in nodal signalling (dorsalising signal during embryogenesis) (Krebs, A Thesis 2010). Defects in this signaling pathway, may be responsible for the loss of floor plate or notochord defects, and could potentially be responsible for the curved and ventralised phenotype and loss of motor neurons observed in this study (Chang LL, and Kessler DS 2010). However it should be noted there are many causes for a curved phenotype, such as the knock down of the transmembrane protein crim 1 which is involved in vascular development (Kinna,G et al 2006), mutations within *muscle segment homobox C (msxC)* (Phillips, B et al 2006) and mutations within the

hedgehog signaling pathway have also been reported to produce a similar bent phenotype (Brand et al 1996). Brand et al identified in their study over 27 genes involved in the body shape of embryos, however this number is now likely to have increased as more pathways have been investigated.

Limitation of this study

There were several limitations in this study, firstly maintaining consistent injection volume. As the amount injected was determined by eye, and the needle tips opened by hand, it was impossible to ensure continuous injection volume per sample. There was also variation between the amount injected per fish in the same sample; this was often due to the needle tip breaking, or embryos accidentally being double injected. A method of combating the inconsistency between samples would be to dispel one pump of the injection solution in to a capillary tube of known diameter and measure the length of tubing the solution fills. This would allow the volume dispelled to be calculated and therefore maintained between samples (Bill.R et al 2009).

Secondly due to the time constraint of manually imaging a large number of embryos per group, ensuring that embryos were imaged at the same developmental stage was not feasible, though by removing all samples from the incubator at the same time development was slowed during imaging. However this could be prevented in future investigation by the application of high throughput imaging technologies, such as those employed by Gehrig. J et al 2009.

Thirdly, Mo injections have been identified to have off target effects such as activation of the p53 cell death pathway which is most obviously observed in the head (Gerety, S and Wilkinson 2010; Eisen, J and Smith, J 2008). This should be

controlled for in future investigations.

Future direction

Future investigation should involve more controls, such as including a Mo for p53 in with the *zzz3* Mo injections, which should inhibit p53 induced cell death caused by any off target effects (Gerety, S and Wilkinson 2010; Eisen, J and Smith, J 2008). Other investigation should focus on identifying if the ATG Mo and the UTR Mo are targeting the same gene. By reducing both ATG and UTR Mo concentration, the phenotypes reported in this report should only be observed when ATG and UTR Mo are co-injected.

It is also important to perform recovery experiments, to determine if the phenotype observed by knocking down *zzz3* was a true event. By injecting *zzz3* Mo along with *zzz3* mRNA, a wild type phenotype should be restored, thus proving the knock down phenotype was a true. As well as further investigation in to the effects of *zzz3* on *NGN-rfp* transgenic embryos, *shh* transgenic fish (with *shh* associated to a fluorescent protein) should also be investigated as *shh* has long been used as a marker of the floor plate, due to its expression in normal floor plate development (Brand et al 1996). This would help determine if zzz3 has any effect on the hedgehog pathway and floor plate development.

In situ hybridization should also be conducted to identify if *zzz3* expression is localised to a particular tissue.

In conclusion, this study suggests but does not confirm that *zzz3* plays a role in midline development and potential disruption in neuronal patterning, with knock down of this gene resulting in a bent phenotype and ventralisation.

Epigenetic studies in a human developmental disorder

By

Amy Amelia Slater

A thesis submitted to the University of Birmingham of the degree of MASTERS OF RESEARCH

This project is submitted in partial fulfillment of the requirements for the award of the MRes'

Abstract

Genomic imprinting has long been implicated as a mechanism of growth regulation. Though most genes are expressed by both alleles, around 100 genes have been classified as imprinted and therefore one allele is preferentially expressed depending on the epigenetic profile of the maternal or paternal allele, resulting in a balance between growth promoting and growth repressing genes. Defects in the epigenetic profiles or simply over expression of one of these imprinted genes, results in developmental disorders such as Prader-Willi/Angelman syndrome (Ch15q11) and Beckwith-Wiedemann (Ch11p15)/Silver Russell syndrome (SRS) depending which allele is affected. This study focused on SRS, a disorder associated with pre- and postnatal growth retardation, investigating whether epimutations at six imprinted loci other than 11p15 had any affect on the disease. By utilising a novel methyl quantative PCR assay the methylation state of *PLAGL1, IGF2R, GRB10, SNRPN, PEG3* and *GNAS* was determined in 40 SRS patients and 26 non-SRS laboratory controls and identified potential epimutations in 30% of the SRS individuals at *PLAGL1, IGF2R* and *GRB10.*

Introduction

Epigenetic modifications are heritable modifications altering gene expression without any alteration to the genetic sequence. These modifications, including histone tail modifications (e.g. acetylation, methylation and phosphorylation) and DNA methylation, can either facilitate or inhibit transcription by altering the chromatin density and/or by regulating proteins binding to the DNA. DNA methylation is a vital control mechanism involved in gene silencing. By the covalent addition of a methyl group to cystine bases in CpG islands, (area of the genome rich in cystine (70-80%) usually found near the promoter region of genes) transcription factors are unable to bind the DNA, thus preventing transcription. Methylated DNA has also been associated in the requirement of methyl binding proteins and subsequently histone deacetylases leading to chromatin remodilling towards a heterochromatin state. This mechanism of silencing has been implicated in X chromosome inactivation, cell differentiation, retroelement suppression and genomic imprinting. (Fritz EL et al 2010; Lim. D and Maher. E 2009). Unlike histone modifications, DNA methylation is only removed during primordial germ cell development, where all DNA methylation is cleared including parental imprinting. Imprinting is then restored during spermatogenesis or oogenesis and maintained throughout embryonic development (Le Bouc Y et al 2010).

Genomic imprinting is a phenomenon of epigenetic regulation identified in the 1980s during experiments involving nuclear transfer in mice embryos (reviewed by Lim, DHK, and Maher, E 2010). Since then, around 100 specific imprinted genes have been identified in the human and most have been associated with embryonic

development and growth. Most genes are expressed biallelically, however expression of imprinted genes is restricted to transcription from either the maternal or paternal allele, providing a balance between paternally expressed genes promoting growth (e.g. *IGF2*) and maternally expressed genes restricting growth (e.g. *H19)* (Butler. M 2009; Lim, DHK, and Maher, E 2010). Imprinted genes tend to be located in clusters across chromosomes, allowing multiple genes to be regulated by control elements known as imprinting centres (IC) (Lim. D and Maher. E 2009). Within these regions of imprinted genes, resides CpG rich differentially methylated regions (DMR). These regions as the name describes, are differentially methylated depending on the parental origin of each allele, and regulate expression of the imprinted genes (for example if the maternal DMR is methylated the gene is repressed, while the paternal DMR will not methylated and therefore the gene is expressed) (Lim, DHK, and Maher, E. 2010; Abu-Amero, S et al 2010).

Examples of Imprinting Disorders

The balance between imprinted genes is carefully regulated to ensure proper growth and development. When this balance is disrupted, it results in overexpression of a once regulated gene, and can lead to imprinting disorders, some of which are described below.

Prader-Willi Syndrome (PWS) (OMIM: 176270)/**Angelman Syndrome (AS)** (OMIM: 105830)

PWS and AS are opposite defects associated with imbalanced expression of imprinted genes at Chromosome 15q11-q13. This cluster contains several

imprinted genes including, paternally expressed genes *MKRN3, MAGEL2, NDN, SNRPN, SnoRNAs* and *UBE3AAS* and the maternally expressed genes *UBE3A* and *ATP10A*, which is normally under control of an IC known as *PWS-AS* IC, methylated on the maternal allele. PWS, was first described in 1956, and is now estimated to occur in 1:10,000-20,000 individuals. Phenotypical features initially present with failure to thrive, feeding difficulties, infantile hypotonia and delayed development followed by an insatiable appetite leading to obesity and low IQ during early childhood (Butler. M 2009). There are several molecular causes for this disorder, such as deletion of the paternal imprinted genes (15%), maternal uniparental disomy (UPD) (25-30%) or paternal imprinting defects (1%), but all result in the loss of the paternally expressed genes. The opposite syndrome, AS, is caused by loss of the maternally expressed genes within the 15q11-13 cluster, either by deletion (<1%), Paternal UPD (7%), maternal imprinting defect (~5%) or mutation of *UBE3A* (11%). AS is characterised by happy demeanour, severe mental retardation and ataxic puppet like movements (Lim. D and Maher. E 2009).

Imprinted Chromosome 11p15.5

Ch11p15 contains two IC. IC1 (*H19* DMR), located telomerically, is methylated on the paternal allele allowing expression of growth promoting *IGF2* and unmethylated on the maternal allele permitting expression of growth restricting *H19*. The methylation of these loci on the paternal allele prevents the binding of a CCCTC-binding factor (CTCF) allowing the downstream enhancer region to access the *IGF2* promoter region. In the maternal allele, CTCF binds the unmethylated DMR redirecting the downstream enhancers to the *H19* promoter (Fig 1A). (Abu-Amero, S et al 2010; Bell AC and Felsenfeld G. et al 2000)

IC2 (*KvDMR1* DMR) located centromerically, is methylated on the maternal allele, allowing transcription of *CDKN1C* and *KCNQ1* and not methylated on the paternal allele, enabling transcription of *KCNQ1OT1* (Fig 1A) (Lim, DHK, and Maher, E 2010, Abu-Amero, S et al 2010).

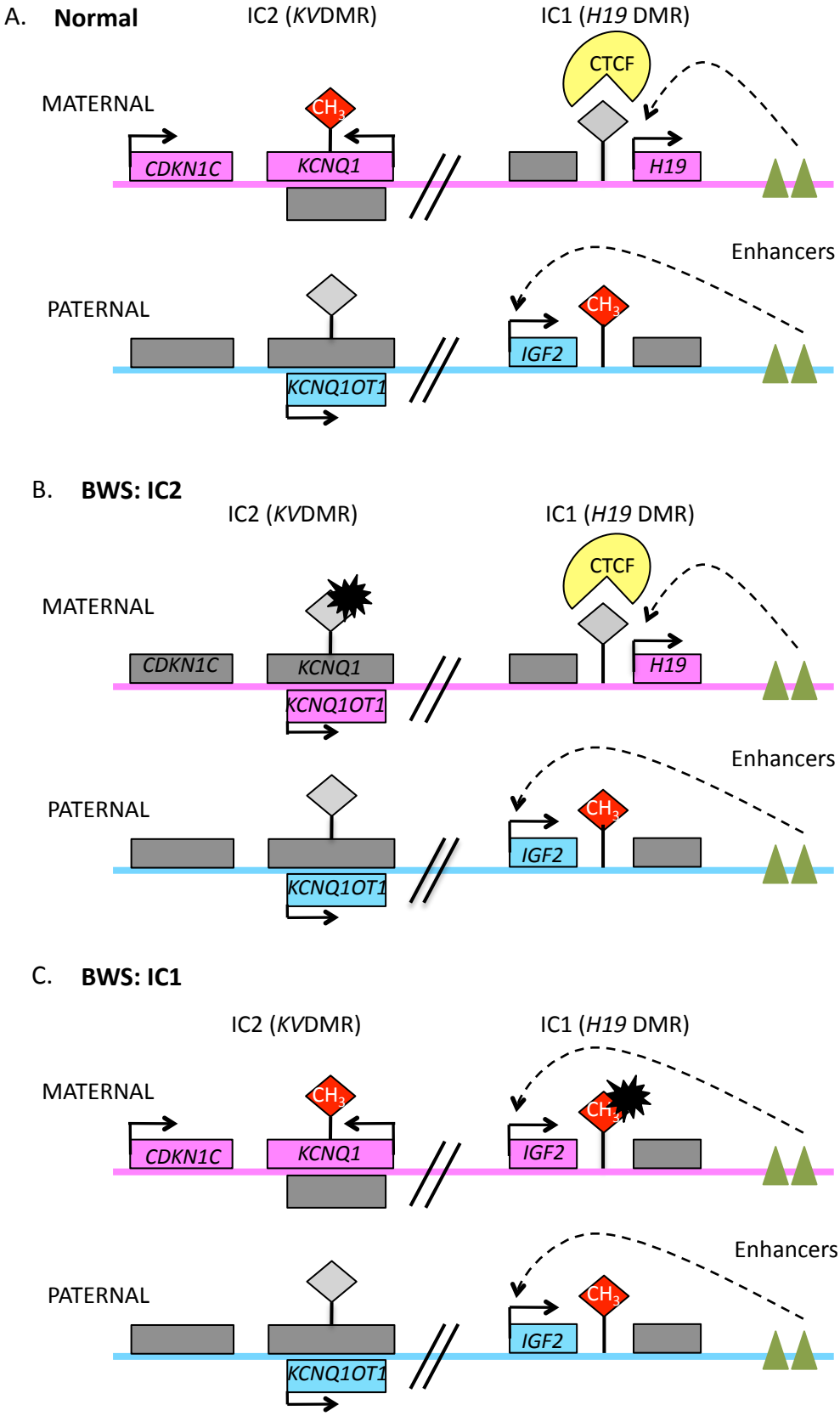
A. Normal
IC2 (KVDMR)
IC1 (H19 DMR)
CTCF
MATERNAL
CH3
CDKN1C
KCNQ1
H19
Enhancers
PATERNAL
CH3
IGF2
KCNQ1OT1
B. BWS: IC2
IC2 (KVDMR)
IC1 (H19 DMR)
CTCF
MATERNAL
CDKN1C
KCNQ1
H19
KCNQ1OT1
Enhancers
PATERNAL
CH3
IGF2
KCNQ1OT1
C. BWS: IC1
IC2 (KVDMR)
IC1 (H19 DMR)
MATERNAL
CH3
CH3
CDKN1C
KCNQ1
IGF2
Enhancers
PATERNAL
CH3
IGF2
KCNQ1OT1

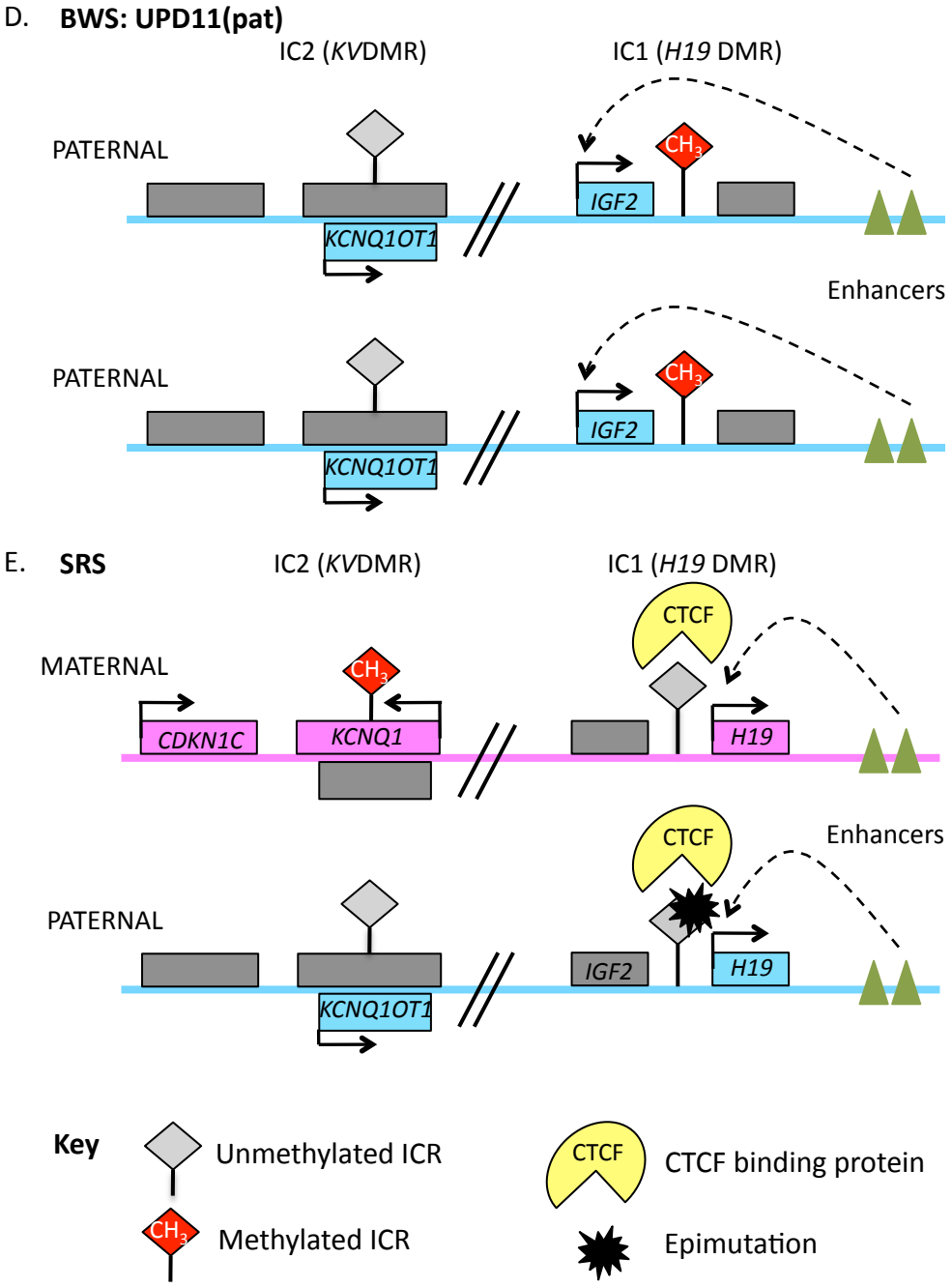

Fig 1: the 11p15.5 imprinting domain. **A)** Normal imprinting. IC1 is unmethylated on the maternal allele allowing binding of CTCF and *H19* expression. While IC2 unmethylated on the paternal allele allowing expression of *KCNQ1OT1.* **B)** BWS IC2 epimutation, methylation of maternal IC2 allows for over expression of paternal gene *KCNQ1OT1* and loss of *CDKN1C.* **C)** BWS IC1 epimutations, gain of maternal methylation of IC1 prevents *H19* and promotes *IGF2*expression. **D)** BWS UPD11(pat) disomy of paternal allele results in loss of all maternally expressed genes. **E)** SRS loss of methylation at the paternal IC1 results in over expression of the maternal gene *H19*.

Beckwith-Wieldemann Syndrome (BWS) (OMIM: 130650)

BWS is an overgrowth disorder believed to occur in 1:13000. Although most cases are sporadic, an autosomal dominant inheritance has been reported in around 10% -15% of cases (Butler. M 2009, Lim. D and Maher. E 2009). The clinical phenotype includes pre- and postnatal overgrowth, macroglossia, hypoglycaemia, abdominal wall defects such as exomphalos in the most severe cases, hemihypertrophy and a significantly increased risk of embryonic tumours (Lim, DHK, and Maher, 2010; BUTLER. M, 2009; Lim, D et al 2009). Molecularly BWS is usually characterised by aberrant expression of paternally expressed *IGF2* or reduced expression of the maternally expressed *CDKN1C* maternally imprinted gene on chromosome 11p15.5. The majority of BWS cases are the result of Loss of Methylation (LOM) at the IC2 (*KvDMR1* DMR), resulting in the decreased expression of *CDKN1C*, and is responsible for approximately 50% of BWS cases, mutations within *CDKN1C* account for 5% of cases (Fig 1B). While at IC1 (*H19* DMR) Gain of Methylation (GOM) resulting in increased expression of the growth promoting gene *IGF2* and loss of *H19* accounts for 2-8% of cases (Fig 1C). Paternal UPD of chromosome 11 accounts for another 10-20% of cases (Fig 1D) although it should be noted that 10-20% of cases have yet to have a cause identified (Abu-Amero, S et al 2010; Lim. D and Maher. E 2009). There is also an association between the cause of BWS and phenotype, with individuals presenting with either UPD11 (pat) or IC1 GOM having an increased risk of developing embryonic tumours, most commonly Wilms tumours (Butler. M 2009). Epimutations within IC2 have been associated with assisted reproductive technologies and increased prevalence of abdominal defects (Lim, D et al 2009).

Silver Russell Syndrome (SRS (OMIM 180860))

SRS was first described in 1953 and is associated with retarded intrauterine and post natal growth (usually <2 standard deviations below the national mean), although head circumference usually gives the impression of macrocephaly. Other features include: feeding difficulties, triangular face with prominent forehead, micrognathia, hemihypertrophy (50% of cases), down turned mouth, and café au lait patches. These features however do not impede life expectancy and become less obvious as the patient grows (Eggermann, T. 2010; Bartholdi, D et al. 2009).

Originally SRS was believed to be independent from BWS and associated with the imprinted gene cluster containing *MEST* and *GRB10* on chromosome 7, due to the identification of UPD7(mat). However it has now been identified that SRS is the opposite of BWS, due to epimutations around 11p15.5 (Lim. D and Maher. E 2009, Eggermann, T et al 2008). UPD7 (mat) has since been identified in only 10% of individuals with SRS, while LOM at paternal IC1 of 11p15 resulting in over expression of *H19* (Fig 1E) is responsible for around 40-60% of cases and maternal disomy of 11p15, is only estimated in 1-2% of cases. Hypomethylation at IC2 has also been reported is SRS, however this is restricted to a few individual cases (Begemann, M et al 2010). Nevertheless for >40% of SRS patients the cause is still unknown (Eggermann, T. 2010; Gicquel, C et al 2005). Investigations conducted by Bliek. J et al. 2006 have proposed that it is the LOM of *H19* that is attributed to the asymmetry observed in SRS, and also identified that this epimutation was present in some cases of isolated asymmetry without SRS. Other groups believe it is the occurrence of mosaicism that results in the asymmetry (Begemann, M et al 2010; Eggermann, T. 2010).

However there are several issues at present that limit investigation of SRS. Firstly diagnosis of SRS; individuals with a weaker phenotype are often missed, and diagnosis is largely dependent on the experience of the clinician. Several scoring systems have now been developed to aid diagnosis (Bartholdi, D et al. 2008,1).

Secondly the presence of mosaicism in SRS, where it has been reported that methylation state differs in different tissues within the same individual (Begemann, M et al 2010; Eggermann, T. 2010), thus increasing the risk of missing vital molecular features during diagnosis and further investigation.

Imprinting disorders and assisted reproductive technologies (ART)

ART has become a more common method of conception since its creation, with it now accounting for 1-3% of worldwide births since 2002. However ART has now been associated with an increase in imprinting disorders, particularly BWS and AS as these are the most intensely studied. There is currently insufficient evidence linking ART to SRS (Owen, CM and Segars, JH. 2009, Lim. D and Maher. E 2009). Lim, D et al 2009 identified that 4% of BWS cases had a history of ART compared to 1.2% in the general population and that these individuals had an increased chance of presenting with LOM at IC2. They also concluded a phenotypical difference between BWS patients conceived by ART compared to those that conceived naturally; for example ART conceived BWS patients had a lower risk of exomphalos but increased risk of non-Wilms tumors, as well as reporting that ART conceived BWS individuals were more likely to present with LOM at DMRs outside of the 11p15.5 region. Although the absolute risk of imprinting defects in ART cases is reported to be <1% (Bowdin S. et al 2007), the mechanism behind this observation with ART is still unclear. It is hypothesised that either the technique

involved with ART or the infertility itself is a factor due to the epigenetic disruption (Lim. D and Maher. E 2009).

Aims and Hypothesised genes linked to SRS

The aim of this study was to investigate the epigenetic profile of SRS patients at a selection of imprinted loci, and to determine if there is any variation in methylation or phenotype between SRS individuals with LOM at *H19* and those with normal methylation. Both studies on BWS patients and patients with TNDM, have shown LOM at other loci (Eggermann, T. 2010; Bliek, J. et al 2009), therefore it is feasible that the same may occur in SRS. The following loci were investigated based on their known role in other imprinted defects:

PLAGL1 (*Pleiomorphic adenoma gene-like 1* (OMIM 603044)) 6q24-q25: Over expression of *PLAGL1* has been implicated in the imprinting disorder Transient Neonatal Diabetes Mellitus (TNDM)(Lim. D and Maher. E 2009). A study by Bliek, J. et al 2009 demonstrated the LOM at both *PLAGL1* and *GNAS* in BWS patients, suggesting that these loci might also be affected in SRS.

GNAS (GNAS Complex Locus, OMIM: 139320) Ch 20q13.3: *GNAS* has been implicated in pseudohypoparathyroidism (Albright hereditary osteodystophy) and is a widely investigated imprinted gene. (Butler. M 2009; Lim. D and Maher. E 2009)

IGF2R (*Insulin Like Growth Factor II Receptor* OMIM: 147280) Ch 6q26: The receptor for the growth promoting *IGF2*, reducing circulating *IGF2* levels and regulating the proliferative effect. *IGF2R* is expressed on only one allele however it is imprinted in a complex manor (OMIM).

GRB10 (*Growth Factor Receptor Bound Protein* OMIM: 601523), Ch7p12.2: *GRB10* was identified as a candidate gene in the region prone to translocation in UPD7 (mat) cases. A mutation in this gene was also reported in a SRS case study (Yoshihashi, H et al 2000.). *GRB10* encodes an adaptor protein that interacts with tyrosine kinase receptors, and is believed to negatively regulate the effects of insulin signaling with loss of *GRB10* resulting in fetal overgrowth (Charalambous M, et al 2003; Abu-Amero, S et al 2010).

SNRPN (*Small Nuclear Ribnucleoprotein Polypeptide N,* OMIM: 182279) Ch15q11.2: *SNRPN* is a maternally imprinted gene involved in RNA processing, with a long tail containing small nucleolar RNAs that are alternatively spliced post transcription; and regulate expression of maternally expressed imprinted genes on the 15q11-13 cluster. Disruption of this gene is associated with PWS (Lim. D and Maher. E 2009; Lim, DHK, and Maher, E 2010), while delinearisation and disruption of Ch15 has been reported in several case studies of SRS (Tamura T, et al 1993; Wilson GN, et al 1985).

PEG3 (*Paternally Expressed Gene 3* 3OMIM: 601483;) C*H19*q13.4: In vivo studies demonstrate that disruption of this paternal gene results in smaller offspring. It was also investigated in a study on atypical PWS subjects (Bale, E et al 2011) and therefore was included in this study.

Method and Materials

Patients

DNA samples were obtained from individuals with suspected SRS for diagnosis, and stored at -80°C until required for further methylation studies. Informed consent had been obtained from all individuals/families.

In this study initial investigation was performed on a cohort of 66 samples (26 non SRS laboratory controls and 40 patients referred for a possible diagnosis of SRS). All of the patient groups had no evidence of UPD7 and a normal karyotype. Prior to the study commencing, 18 of the SRS group were identified during diagnosis to have LOM at *H19* DMR (11p15.5) and the other 22 had normal *H19* DMR methylation.

Upon retrieval, genomic DNA samples were vortexed and centrifuged. Samples were then diluted 1:10 in distilled nuclease free water (dH_20) in separate eppendorf tubes to a total volume of 20µl ready for quantification by Nanodrop spectrophotometer ND-1000. Nanodrop quantification was employed not only to determine genomic DNA concentration, but also to evaluate purity by observing the 260/280 and 260/230 ratios, both of which should be greater than 1.80. If either ratio were lower than the stated threshold it would indicate the presence of protein, phenol or other contaminants and could degrade the genomic DNA or affect the activity of the restriction enzymes used in the methylation studies. Poor quality DNA was excluded from this study. (Thermo scientific NanoDrop 1000 Spectrophotometer manual *http://www.nanodrop.com/Library/nd-1000-v3.7-users-manual-8.5x11.pdf*)

Methylation Studies

All methylation analysis was performed using the EpiTect Methyl qPCR Assay (SAbiosciences Qiagen) following the protocols provided and summarised below. The Assay works on the principle of digesting genomic DNA with either methylation sensitive or methylation dependent enzymes followed by quantification of the remaining undigested DNA by real time PCR (qPCR) providing an indication to the methylation state of the CpG region investigated. The benefit of this assay over other techniques traditionally employed to detect DNA methylation, such as bisulfite sequencing and methylation specific PCR, is the reduced time constraints, simple technique with a semi high throughput, reliablility, and all samples are internally controlled excluding the need to run controls in the PCR such as house keeping genes. As each assay is predesigned, there is also no need for PCR primer design or optimisation.

Digests

Firstly DNA methylation digest was conducted using a Methyl-Profiler Enzyme kit (MeA-03 SAbiosciences Qiagen). In summary a master mix of input DNA was created consisting of 26µl 5X Digestion Buffer, 0.5µg Genomic DNA and dH_2O added to a final volume of 120µl, before mixing by vortex. Four digests were set up per master mix solution in a 96 well plate (12 patients per plate)

1) **Mock digest (Mo):** dH_2O was added instead of restriction enzymes, to the genomic DNA, therefore representing the total volume of input ingredients and acts as the input control for the qPCR
2) **Methylation Sensitive Digest (Ms)**: Genomic DNA master mix was added to a methylation sensitive enzyme that only digests unmethylated and

partially methylated DNA. This ment that during qPCR hypermethylated DNA would be amplified and quantified.

3) **Methylation Dependent Digest (Md)**: Genomic DNA master mix was added to a methylation dependent enzyme that preferentially digests methylated DNA. This ment that during qPCR unmethylated DNA would be amplified and quantified.
4) **Double Digest (Msd)**: Both methylation sensitive and methylation dependent enzymes were incubated with the genomic DNA master mix, digesting the entire DNA. This control was included to quantify the background noise during the qPCR.

It was important that for each digest the same amount of genomic DNA was added to avoid a biassed or inaccurate result during the PCR. Samples were sealed then incubated on tetrad PCR machine at 37°C for 16 hours, followed by 20 minutes at 65°C to denature and inactivate the digestion enzymes. The stock DNA digests were then stored at -20°C until required for PCR, when defrosted samples were briefly centrifuged, before required volumes of samples were aliquoted out onto to PCR plate. To ensure digestion was complete the assay was designed so that each sample was incubated for longer than needed and had an excess of restriction enzyme.

PCR

To determine the methylation status of specific loci, qPCR was performed using predesigned and pre-optimised methyl-profiler DNA methylation qPCR primers. PCR master mix was created following the instructions in the manual. Each well was analysed by PCR consisting of RT^2 SYBR Green PCR Sensi mix (includes

Hotstart DNA polymerase), dH_2O, restriction enzyme digest (Mo, Ms, Md, Msd) and optimised methyl-profiler DNA methylation qPCR primer set, for the specific CpG island of investigated loci. Following vortexing and a brief spin down PCR was run on Bio-Rad I cycler IQ5 qPCR machine with the following program (Table 1)

Table 1: q-PCR cycle program

Cycles	**Temperature**	**Time**
1	95°C	10 minutes
3	99°C	30 seconds
	72°C	1 minute
40	97°C	15 seconds
	72°C	1 minute
Melt Curve	Set according to machine	

The Initial 10 minute cycle 1 was required to activate the Hot Start DNA polymerase to allow successful amplification of DNA. The melt curve analysis was included as a control to ensure complete PCR amplification. After completion of the PCR, Ct values were collected for analysis of methylation state. The assay provided a predefined analysis spreadsheet that determined the percent of DNA that was hypermethylated (HM, >60% methylated), unmethylated (UM, 0% methylated) and intermediately methylated (IM, between 0 and 60% methylated)

in relation the Ct value of the mock digest minus the double digest (Background noise). The statistical analysis employed also calculated the efficiency of the enzyme digest setting the threshold for successful digests at 75% of DNA digested (EpiTect Methyl qPCR assay Manuel http://www.sabiosciences.com/support_manual.php?pfamily=dnamethylation).

This methylation study looked at the HM levels of up to 40 SRS (proven or suspected) patients compared to controls (n=26) at various imprinted loci that might, based on previous literature, represent potential areas of altered methylation in SRS. Loci investigated and primer locations are listed in Table 2.

Table 2: qPCR primer location and target gene. Sequence was not disclosed.

GENE	**Cytogeneic location**	**CpG island location**	**Assay position (central point)**	**Associated imprinting disorder**
PLAGL1	Ch6q24-q25	Ch6: 144370609-144371540	Ch6: 144371270	TNDM
IGF2R	Ch6q26	Ch6: 160426265-160427502	Ch6: 160427151	Potentially involved in SRS
GRB10	Ch7p12.2	Ch7: 50849753-50850871	Ch7: 50850409	Potentially involved in SRS
PEG3	C*H19*q13.4	C*H19*: 62043812-62044146	C*H19*: 62044146	-
SNRPN	Ch15q11.2	Ch15: 22751128-22752147	Ch15: 22751228	PWS
GNAS	Ch 20q13.3	Ch20: 56861703-56861911	Ch20: 56861806	Albright hereditary osteodystophy

Data Analysis

LOM or GOM was classified as any HM value either 2 standard deviations (SD) below or above the mean of all SRS patients and controls respectively. Ensuring at least a 95% confidence for controls. All samples that showed apparent LOM or GOM at any loci or individuals with an IM value greater than 5.5% were repeated, to ensure the result was true.

All data analysis was conducted using Excel2008 and GraphPad Prism software. Methylation data is presented with mean ± SEM displayed. Statistical tests conducted included Students t-test and Chi-squared, Fisher's Exact Tests and Pearsons correlation co-efficitent.

Results

Comparison of clinical features

The first step in this study was to determine if there was any correlation between the presented clinical features and the known molecular information obtained during diagnosis. All individuals included in this study presented with short stature and had been suspected of having SRS. During diagnosis genetic abnormalities and UPD7 had been excluded in all cases. The available clinical data for each of the case subjects is presented in Appendix 1.

The clinical features of patients with and without LOM at *H19* were compared (see Table 1). Features such as hemihypertrophy, prominent forehead, down turned mouth, fifth figure clinodactyly and micrognathia appeared to be more frequently observed in SRS individuals with *H19* LOM than those without this LOM (see Table 1 and Figure 1). This suggests that individuals with *H19* LOM are more likely to present with clinical features of SRS and possibly a more severe phenotype than with normal *H19* methylation (Table 3 and Fig 2).

It should be noted that for phenotypical analysis case SRS 18 was excluded, as initially the patient was suspected of having BWS, however atypical BWS features, including unsteady gait, provoked further investigation and uncovered evidence of *H19* LOM during molecular genetic analysis. This was contradictory to the expected result for BWS where hypermethylation of the 11p15.5 loci is usually observed, and suggests a molecular diagnosis of SRS, allowing this individual to be included in the subsequent methylation studies.

There was no difference in the frequency of children conceived by ART in the two SRS groups (two in each group), however, the overall frequency of ART births within the SRS population (10.2%, (4/39) if SRS18 is excluded and 12.5% (5/40) if SRS18 is included) was higher than expected, as the expected frequency of an imprinting condition in ART births in the UK population is approximately 1% (Lim et al 2009).

It has previously been reported that the frequency of ART births is increased in BWS children (in particular those with LOM at KvDMR1), that there are phenotypic differences between ART-conceived and naturally conceived BWS children and that ART-conceived BWS children are more likely to have hypomethylation outside 11p15.5 (Lim et al 2009). These observations raised several questions. Firstly, do SRS patients also show evidence of hypomethylation at other imprinted loci outside 11p15.5? Secondly, if hypomethylation is observed, are there differences in frequency between those with and without *H19* LOM and does this influence phenotype?

Table 3: Summary of the clinical data of all Silver Russell patients tested

		Silver Russell Clinical data			
		All	*H19* Normal	*H19* LOM	P Value
	Number of cases	39	22	17	-
Sex	Male	13/39	7/22	6/17	-
	Female	20/39	12/22	8/17	-
	Unknown	6/39	3/22	3/17	-
	Normal karyotype	39/39	22/22	17/17	-
	UPD7	0/39	0/22	0/17	-
	H19 LOM	17/39	0/22	17/17	-
ART conception		4/39	2/22	2/17	-
Pregnancy					
	Preterm (<37 weeks)	11/39	6/22	5/17	-
	Term (37-41 weeks)	28/39	16/22	12/17	-
Prenatal period (<1 month)					
	Intensive care	18/39	7/22	11/17	0.056
	Feeding difficulties	20/39	11/22	9/17	1.000
	Hypoglycaemia	6/39	2/22	4/17	0.374
Postnatal period (>1 month)					
	Feeding difficulties	23/39	14/22	9/17	0.531
	nasogastric tube	7/39	5/22	2/17	0.438
	Gastromy fed	2/39	1/22	1/17	1.0000
	Hypoglycaemia	3/39	0/22	3/17	0.074
	Café au lait patches	6/39	4/22	2/17	0.679
	Visual defects	3/39	2/22	1/17	0.374
	Mental retardation	11/39	7/22	4/17	0.725
Other features					
	Hemihypertrophy	17/39	6/22	11/17	**0.026**
	Delayed bone age	7/39	5/22	2/17	0.438
	Facial asymmetry	9/39	4/22	5/17	0.465
	Prominent forehead	27/39	11/22	16/17	**0.005**
	Down turned mouth	17/39	5/22	12/17	**0.004**
	Dental crowding	1/39	0/22	1/17	0.436
	Micrognathia	8/39	3/22	5/17	0.261
	Fifth finger clinodactyly	24/39	10/22	14/17	**0.024**
	Congenital cardiac malformations	6/39	4/22	2/17	0.679
	Camptodactyly	2/39	0/22	2/17	0.183

Clinical features numerically summarised, comparing Patients with *H19* LOM SRS and *H19* normal SRS individuals. Statistical difference between the two SRS groups was determined by Fisher extract tests. P values in bold are significant

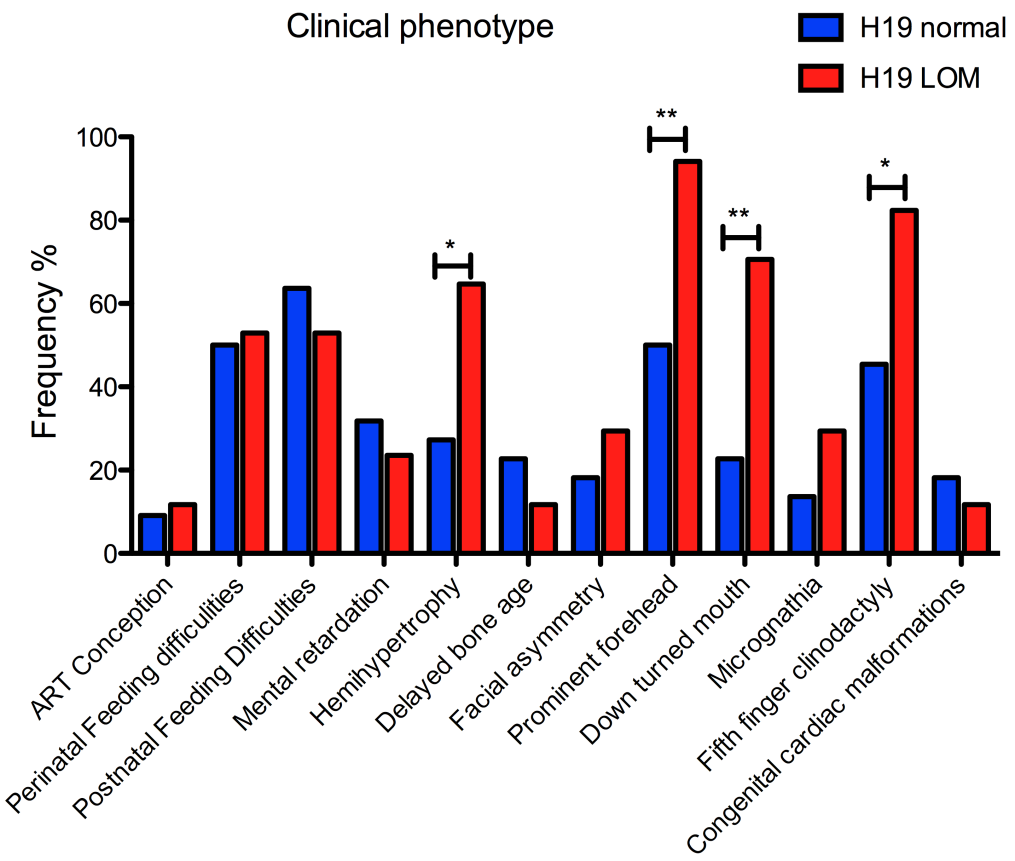

Fig 2: Graphical representation of the clinical data provided with the SRS patients. Frequency of each phenotype was calculated as a percentage of the total group allowing comparison of H19 LOM SRS population and The H19 normal SRS population. Statistical analysis, Fisher extract test conducted *=<0.05, **=<0.01

Methylation state at imprinted loci in SRS patients

Investigation of the methylation at imprinted loci other than *H19* was conducted using EpiTect Methyl qPCR Assay on DNA from 26 non-SRS controls and 40 SRS cases previously described.

The methylation state of the following imprinted genes was determined and comparison was made for the results between (a) controls and (b) the SRS group (Fig 3 A-E).

Mean HM percentage at *PLAGL1*, *IGF2R*, *GRB10*, *SNRPN* and *PEG3* was not significantly different between control and SRS. Further inspection of the distribution of methylation between the control and SRS groups revealed evidence of outliers at some loci thus indicating potential methylation variation between SRS patients and the normal population.

Interestingly *PEG3* showed high variability in methylation within the control group and displayed potential clustering of sub populations. The high variability within the control population prevents any conclusion being drawn about the methylation status of this gene in SRS.

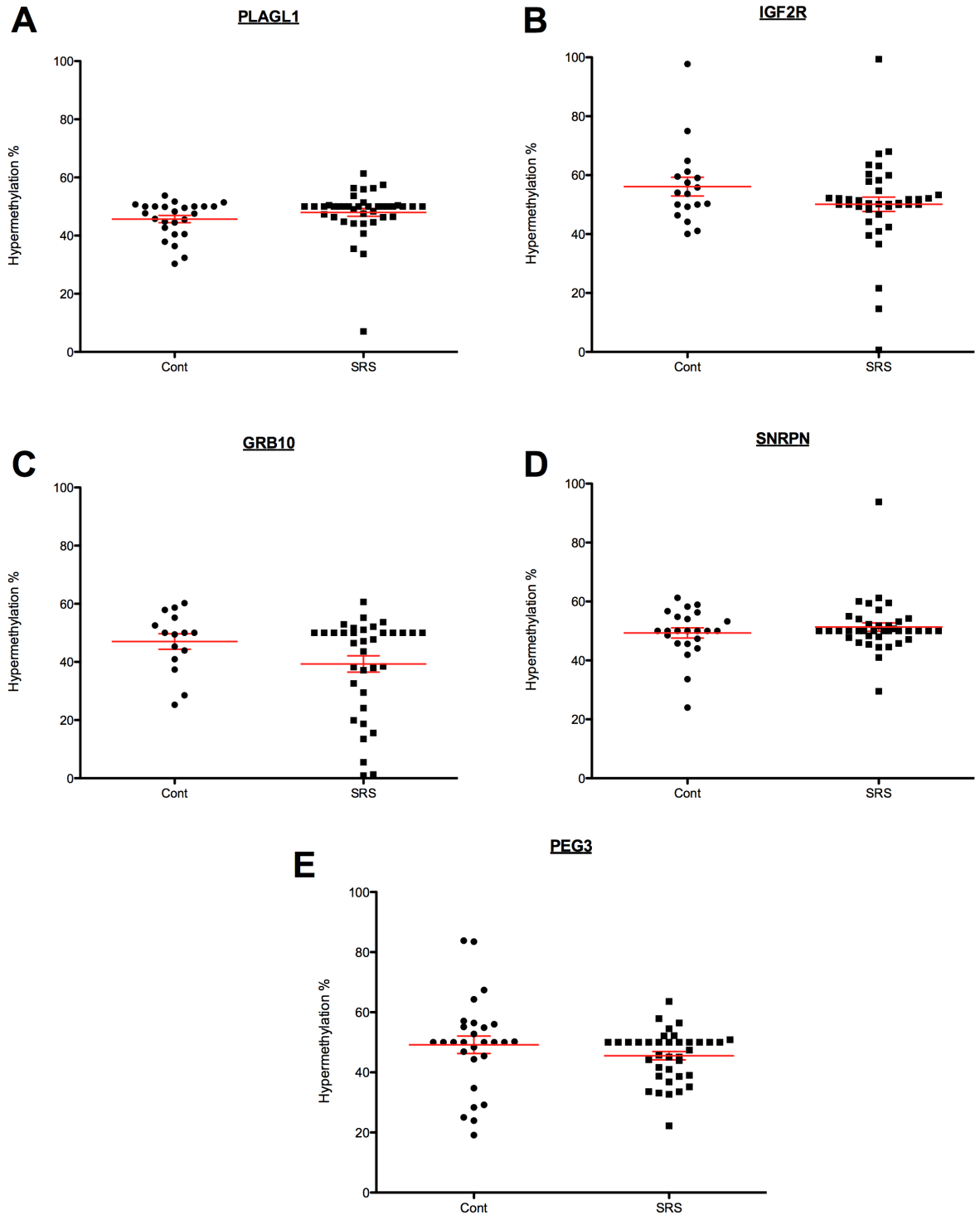

Fig 3: Comparison of HM percentage between control and SRS populations at imprinted loci. In several loci A) *PLAGL1,* B)*IGF2R,* C)*GRB10* and D) *SNRPN* SRS population contains outlying methylation states. Red lines indicate means ± SEM Statistical analysis, Student T-test conducted but no significant difference.

Imprinted loci methylation state in *H19* LOM and *H19* normal SRS cases

To establish if the SRS methylation outliers reported in Fig 3 are significant and localised to either the *H19* LOM SRS or the *H19* normal SRS population, the data was re-analysed, separating the two sub populations (Fig 4). Further analysis showed that all outlier values were found in SRS patients with *H19* LOM.

Mean HM percentage at *IGF2R* (P=0.04) and *GRB10* (P= 0.003), in *H19* LOM SRS population was significantly lower than control population.

Most *H19* LOM individuals however have a HM value for *IGF2R* on trend with norm. The reduced average could therefore be attributed to three outliers that showed large amount of LOM (Fig 4B) indicating that most cases of *H19* LOM SRS are not associated with epimutation at *IGF2R* loci.

GRB10 however (Fig 4C) presented the most interesting pattern of methylation. Potential clustering into 4 groups was observed within this population, with one cluster showing almost complete LOM. This pattern of clustering was not observed in the *H19* normal SRS population and two clusters were seen within the control population. The implications of this observation have yet to be determined and a larger cohort of individuals should be examined to determine if this is a true observation.

A preliminary study of *GNAS* was also conducted on *H19* LOM SRS and 14 controls, however technical issues prevented investigation of this locus on *H19* normal SRS, so no conclusions as to methylation state can be drawn (Fig 4F).

Nevertheless it does appear that within the *H19* LOM SRS population there are 2 outliers with increased methylation, though further investigation is required.

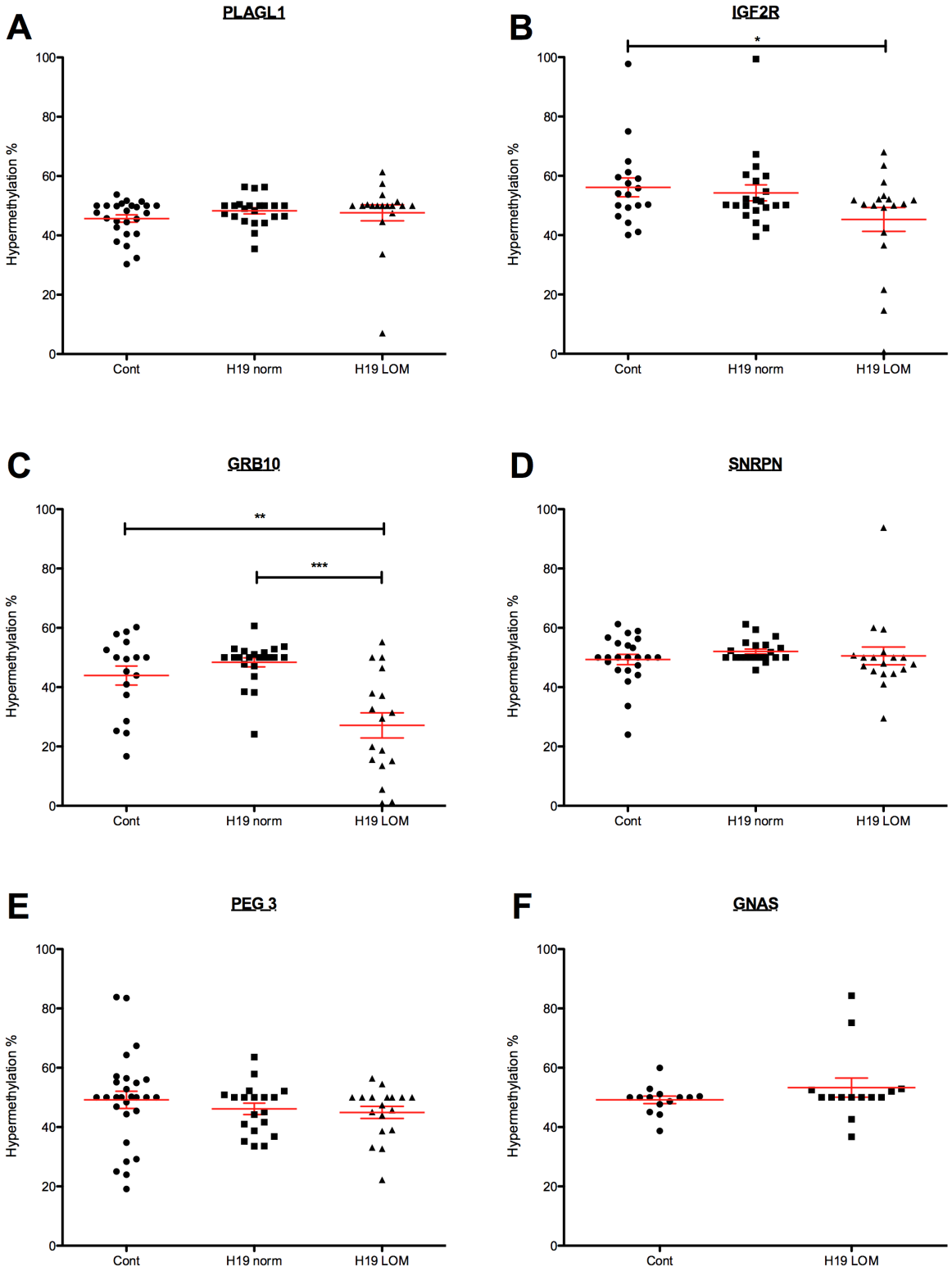

Fig 4: Comparison of HM percentage between control, *H19* normal methylated SRS and *H19* LOM SRS populations at imprinted loci. All SRS individuals with outlying methylation states are located in the H19 LOM SRS. Red lines indicate means ± SEM Statistical analysis, Student T-test conducted *=<0.05, **=<0.01 ***=<0.001

Correlation between methylation states of imprinted loci

Investigation was conducted to identify any correlation between imprinted loci and their methylation state (Fig 5). No correlation between the methylation states of loci was identified, however when determining the Pearson's correlation for each locus, *PLAGL1* vs. *IGF2R* (Fig5A) for the *H19* LOM SRS population showed a significant correlation (r= 0.49 P value= 0.03). Upon exclusion of the outlier (case SR18) no significant correlation (r= -0.21 P values=0.39) was calculated, indicating that case SR18 skewed the data.

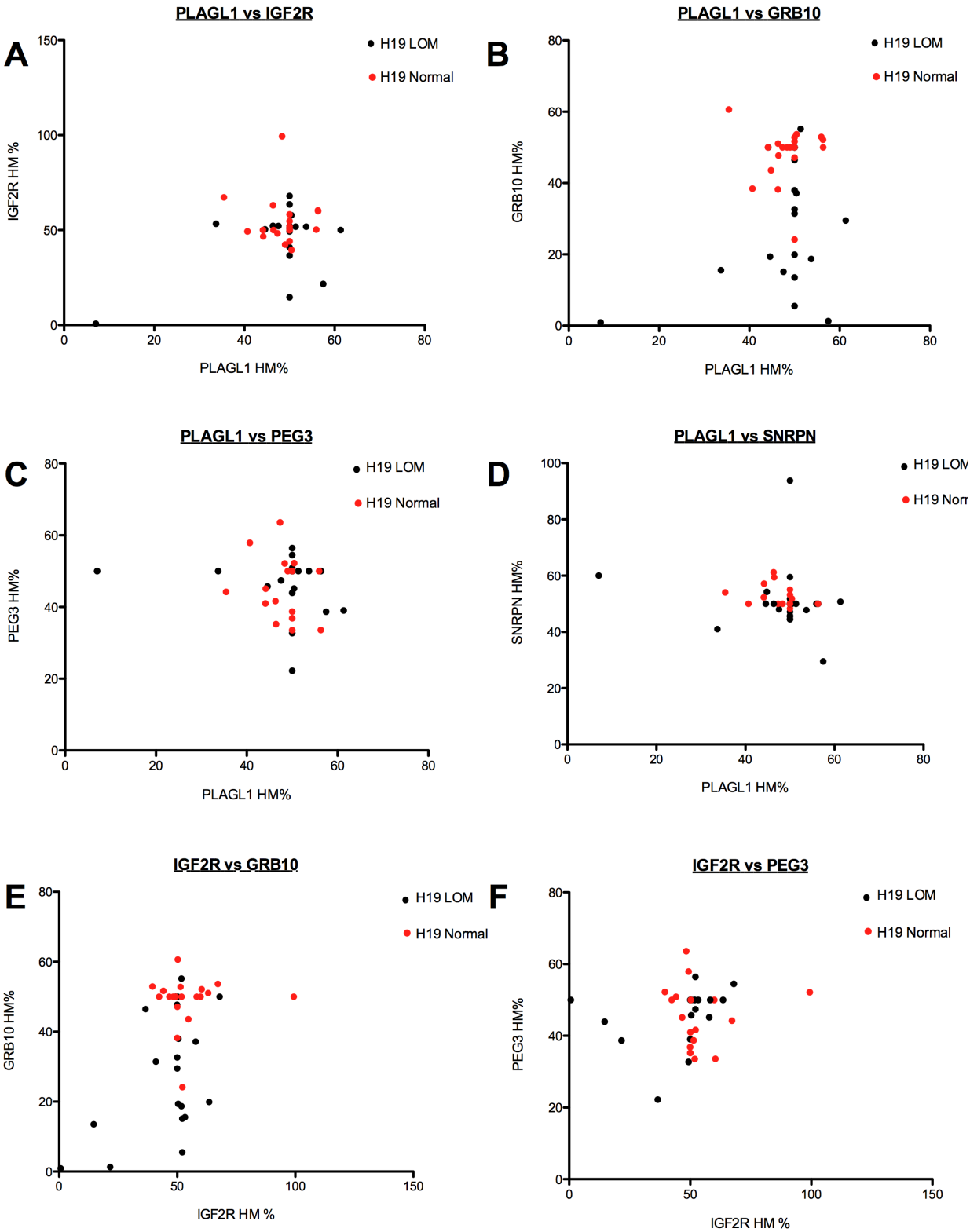
PLAGL1 vs IGF2R
A
H19 LOM
H19 Normal
IGF2R HM %
PLAGL1 HM%
PLAGL1 vs GRB10
B
GRB10 HM%
PLAGL1 vs PEG3
C
PEG3 HM%
PLAGL1 vs SNRPN
D
SNRPN HM%
IGF2R vs GRB10
E
IGF2R HM %
IGF2R vs PEG3
F

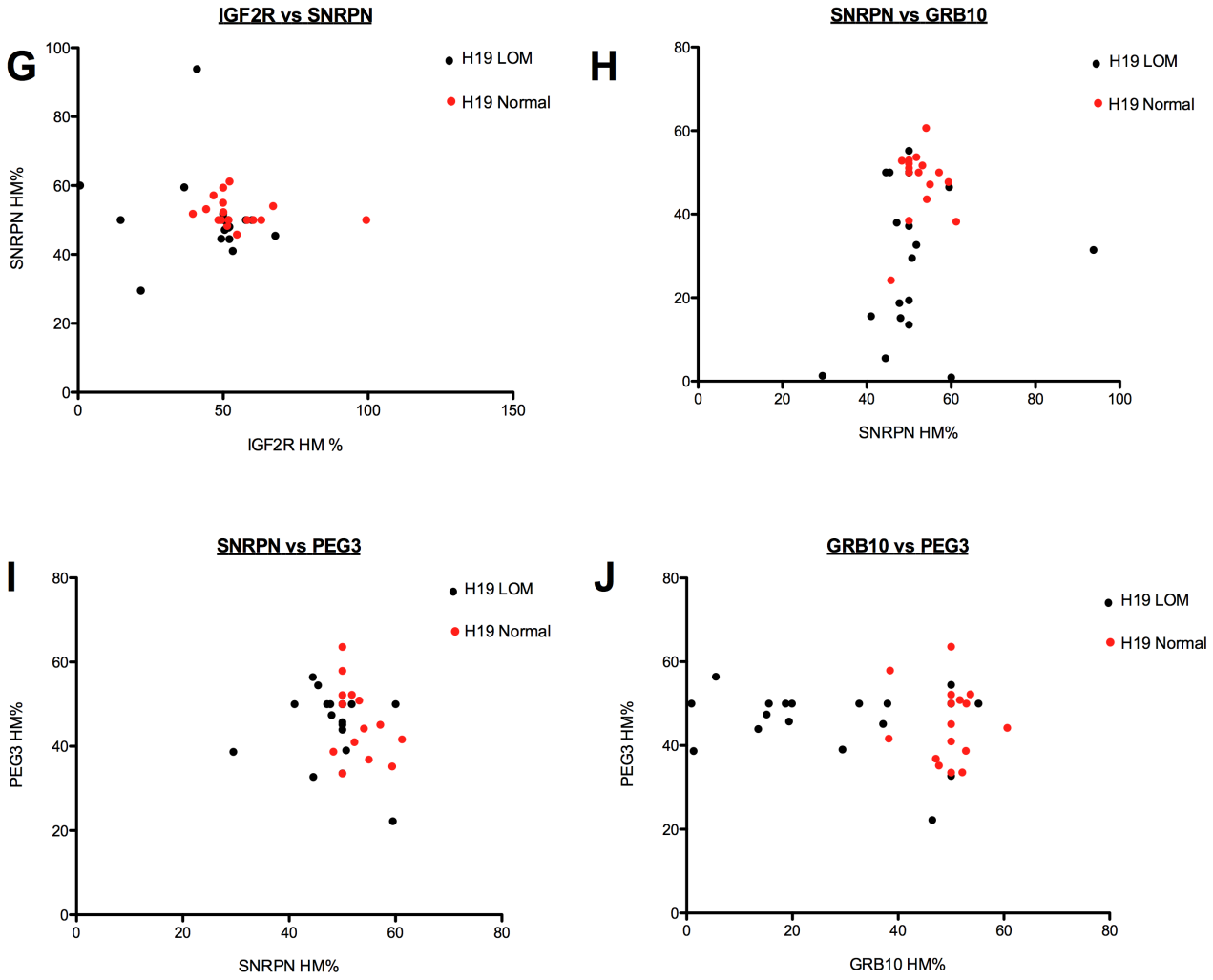

Fig 5: Investigation of any correlation between the methylation sate between loci. Pearson correlation coefficient was conducted to identify any statistical correlation.

Linking epimutations to phenotype

Identification of the frequency of epimutations within the *H19* LOM and *H19* normal SRS populations was calculated (Fig 6). Though no trend was apparent when comparing the frequency of GOM epimutations between the two SRS populations, investigation in to LOM (FIG 6B) identified a possible trend. LOM at one or more additional loci (excluding *H19*) was significantly more frequent (Fisher exacts test P=0.03) in the population of SRS individuals that already had LOM at *H19* (33% of individuals tested), than those with normal methylation at *H19* (4% of individuals tested had LOM at other loci). There was also one *H19* LOM SRS case (SRS18) presenting with LOM at 3 loci (*GRB10*, *IGF2R* and *PLAGL1*), providing a strong case that epigenetic alterations at non-11p15.5 imprinted loci can influence the phenotype of patients. HM levels of individuals presenting with epimutations are presented in table 4.

Comparison of clinical data of individuals with LOM at one locus identified no specific phenotype that could be attributed to the epimutations observed. This finding was also observed for cases with GOM epimutations.

Given the association with imprinting disorders and ART, conception method was then assessed in all cases with either LOM or GOM at one of the investigated loci. The results indicate that there was no association between methylation state and conception with only 1 case per methylation group being conceived via ART.

Cluster analysis was performed to identify any less apparent associations between methylation state and individuals. (Fig7) As *H19* was previously

determined during diagnosis by alternative techniques, the exact methylation value is unknown and not included in the cluster analysis. This analysis highlighted 3 distinct groups. Group I consisted of n=7 all of which fall within the *H19* LOM SRS group. Group II consisted of n=28, Group III contained n=4, 1 of which was from *H19* LOM SRS population. This analysis suggests there maybe is some association between individuals, however phenotypical analysis of these groups does not yield any clear associations.

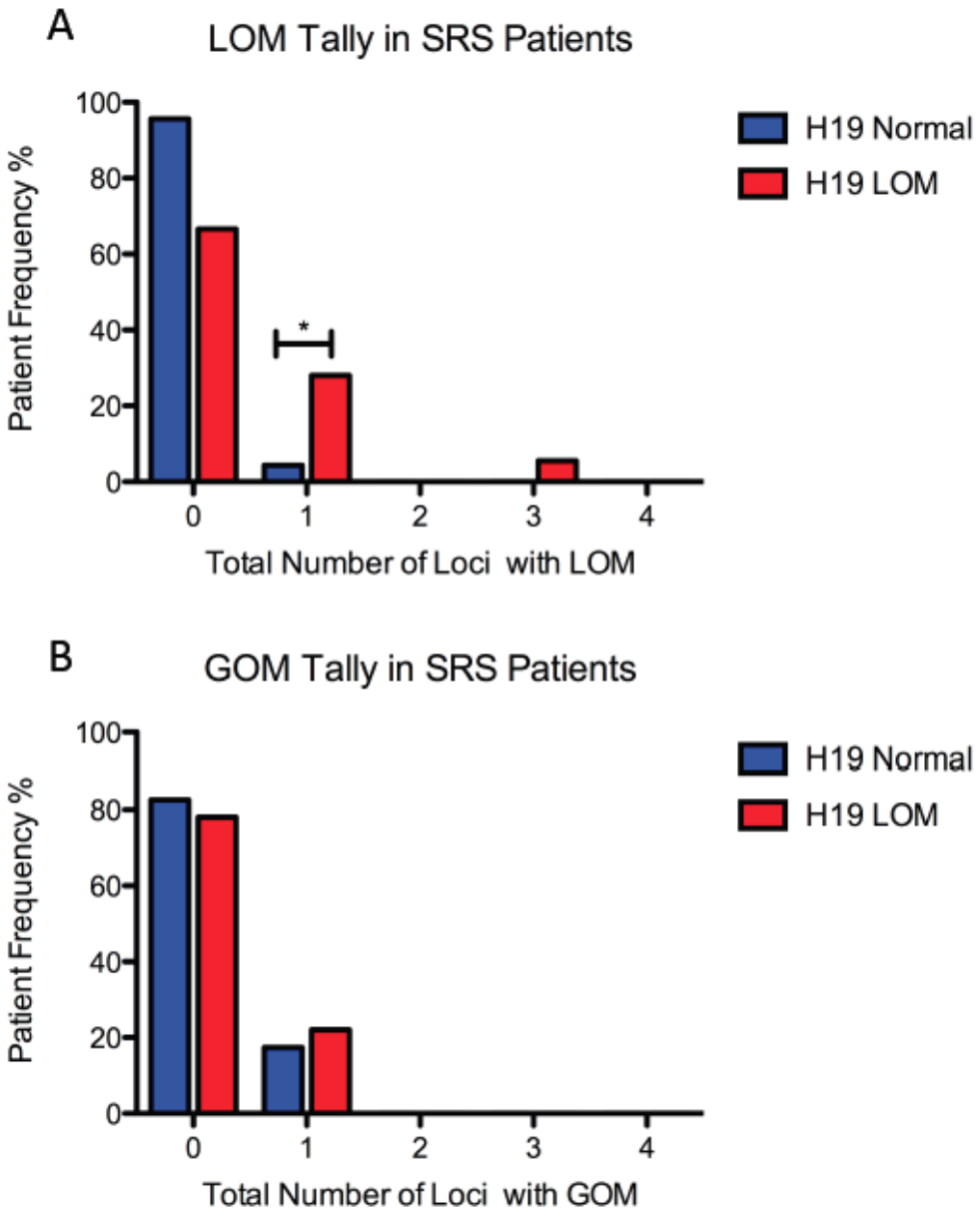

Fig 6: Frequency of epimutations in SRS normal and SRS *H19* LOM population. A) Frequency of individuals presenting with LOM at loci other than *H19*. B) Frequency of individuals presenting with GOM at loci other than *H19.* Fishers exact test conducted to determine significance between the two SRS populations *= < 0.05

Table 4: HM levels of individuals presenting with epimutations							
Case	*H19* status	Pecentage of HM at loci					
		PLAGL1	***GRB10***	***GNAS***	***PEG3***	***SNRPN***	***IGF2R***
SR6	LOM	50.00%	31.44%	50.00%	N/A	**93.78%**	40.95%
SR8	LOM	50.00%	**5.52%**	50.00%	56.43%	44.44%	52.15%
SR9	LOM	**61.34%**	29.47%	25.95%	39.02%	50.72%	50.00%
SR10	LOM	50.00%	13.52%	52.49%	43.95%	50.00%	**14.64%**
SR11	LOM	**57.46%**	**1.29%**	50.00%	38.67%	29.51%	21.62%
SR12	LOM	**33.69%**	15.55%	50.00%	50.00%	41.01%	53.32%
SR15	LOM	50.00%	46.45%	42.64%	**22.22%**	59.51%	36.60%
SR18	LOM	**7.05%**	**0.91%**	**84.29%**	50.00%	60.03%	**0.67%**
SR32	Norm	**35.46%**	60.65%	N/A	44.20%	54.06%	67.23%
SR34	Norm	48.35%	50.00%	N/A	52.13%	50.00%	**99.35%**
SR35	Norm	**56.31%**	52.13%	N/A	33.58%	50.00%	60.38%

Percentage of HM for each investigated loci. Thershold for LOM or GOM was determinded values <2SD above or below the overal mean HM value. **Bold red text**= LOM **Bold Blue text**= GOM

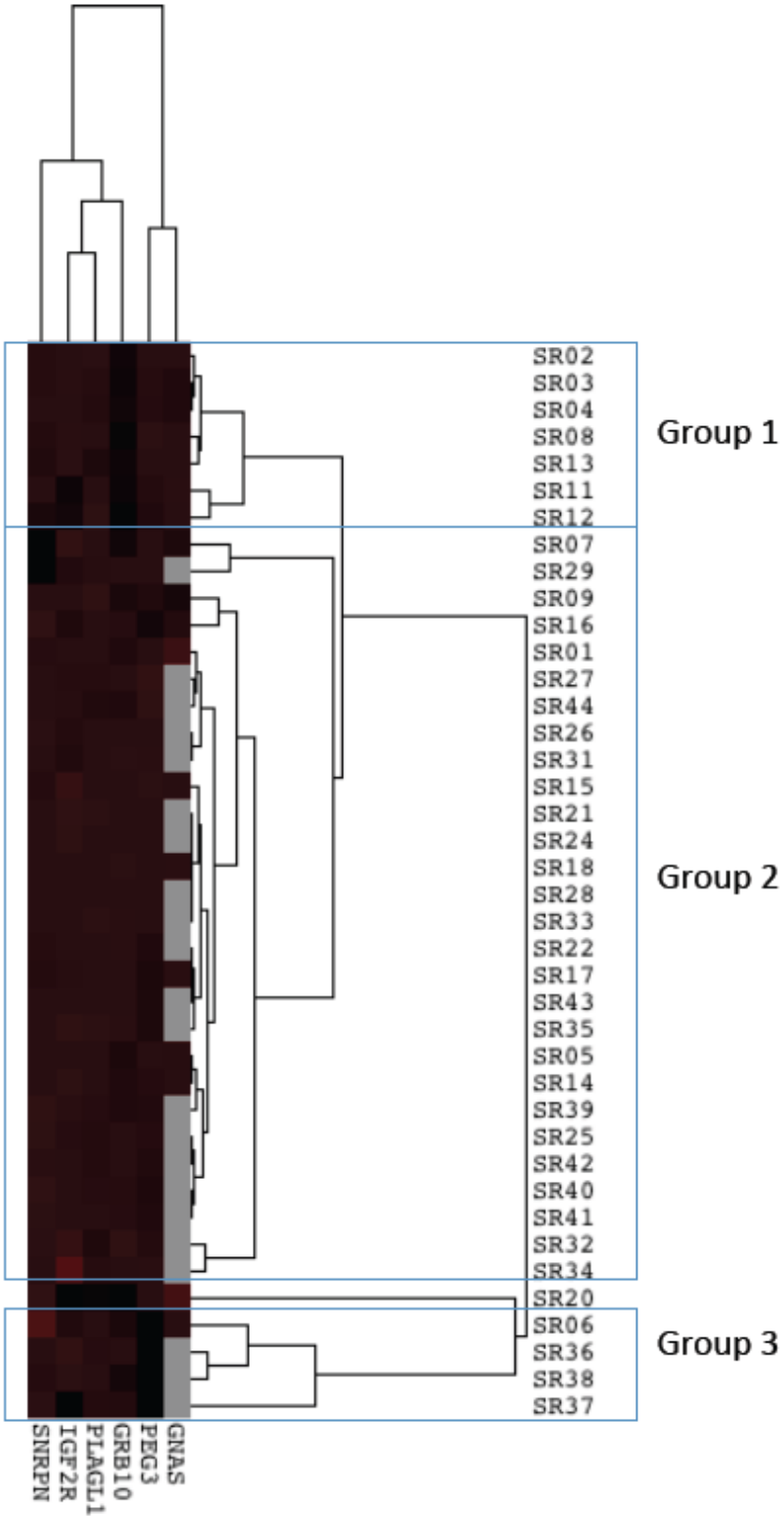

Fig 7: Cluster analysis of all HM% obtained at *GNAS, PEG3, GRB10, PLAGL1, IGF2R,* and *SNRPN.* Three main clusters are observed, with most individuals residing in Group 2. Group 1 and 3 could possibly indicate an alternative non molecular association between the grouped individuals , although no phenotypical link had been observed.

Discussion

The aim of this study was to investigate the association between SRS and methylation state at a selection of imprinted loci. The overall findings showed individuals with SRS are more susceptible to epimutations at imprinted loci other than *H19* compared to the control population. SRS individuals that present with *H19* LOM are also more likely to have LOM at other loci compared to SRS patients with normal IC1 11p15.5 methylation.

Findings and observations

It was observed during this study that patients with LOM at the *H19* loci were more likely to present with more severe SRS phenotype, including increased prevalence of hemihypertrophy, prominent forehead, fifth figure clinodactyly and other abnormalities associated with SRS. This discovery is consistent with the findings of Bruce.S et al 2009; Bartholdi D, et al 2009 and Wakeling EL et al 2010, where the phenotypes of SRS patients idiopathic, UPD7(mat) and LOM *H19* were compared in larger cohorts (42 confirmed SRS patients, 201 patients with suspected SRS and 64 confirmed SRS respectively). Bruce et al. additionally report that individuals with extreme *H19* LOM (<9% methylation) also presented with skeletal abnormalities (spinal problems) and genital defects. However for our study there was no clinical data about these abnormalities nor the degree of methylation of *H19*. Quantification of *H19* methylation would allow future investigation into whether extreme hypomethylathion of *H19* individuals is associated with increased LOM at other loci.

This study identified the presence of either GOM or LOM epimutations at loci other than *H19* in 12 of the 40 (30%) SRS individuals. 33% of patients with hypomethylation at *H19* loci presented with LOM at other imprinted loci compared to 4% of patients with normal *H19* methylation. This corroborates the findings of Azzi at al.2009 and Turner, CLS et al 2010 and where it was reported that individuals with *H19* LOM displayed multilocus methylation defects. However our study identified this to be a more common occurrence than Azzi et al. 2009 and Turner, CLS et al 2010 where it was reported that 9.5% and 17% (respectively) of individuals with *H19* LOM had LOM at least one other imprinted loci. However studies by Schönherr N et al, 2007 and Peñaherrera, M. et al 2009, on 32 and 35 SRS patients respectively, provided no evidence of abnormal methylation at other imprinted loci. There was no association observed between phenotypes in individuals with LOM at multiple imprinted loci in our study, mirroring the results of Azzi.S et al 2009.

Six imprinted loci were investigated in the study, *PLAGL1*, *IGF2R*, *GRB10*, *PEG3*, *SNRPN* and *GNAS*. 3 SRS individuals with LOM and 4 with GOM at *PLAGL1* were identified; this result does not present a distinct conclusion being drawn as to the state of methylation in SRS. It has been shown that *PLAGL1* and *GNAS* are hypomethylated in several BWS patients, Bliek, J et al 2009 and therefore could potentially be affected in SRS, however a multiloci study on SRS patients did not yield any change in *PLAGL1* methylation.

One of the most interesting loci with aberrant methylation identified in this study was *IGF2R*, where 2/18 (11%) SRS with *H19* LOM demonstrated LOM at

this locus. This is contradictory to a study by (Turner, CLS et al 2010), where 2/23 *H19* LOM and 5/56 *H19* norm SRS paitents presented GOM at this loci. Th author hypothesised that GOM increased expression of *IGF2R*, which in turn decreases circulating *IGF2* and decreasing growth. However this study also identified 1 *H19* LOM SRS individual with LOM at *IGF2R*, while another in multi loci study, only identified LOM as the epimutation present at this locus (Azzi et al 2009), which is consistent with the finding of the current study. As DNA methylation is normally associated with reduced gene expression, one would hypothesise that LOM at *IGF2R* would result in increased gene expression, and therefore decreased *IGF2* and subsequently reducing growth. OMIM (♯14728) summarised that loss of *IGF2R* in mice results in fetal over growth.

The other finding was LOM at the *GRB10* locus in 3/17 *H19* LOM. Though there were a few individuals in the control population that expressed a slight decrease in methylation, this degree of LOM was not as strong as that observed in the 17% of SRS *H19* LOM mentioned. LOM was also observed in one individual involved the multi loci study performed by Turner, CLS et al 2010, however this study did not expand on the finding, and instead concluded that epimutations at candidate imprinted genes *MEST*/*PEG1, GRB10* and *PEG10* on Chromosome 7 may not lead to an SRS phenotype. LOM at this locus would also result in increased gene expression. A previous study on mice identified that maternal over expression of *GRB10* (which also is observed in UPD7 (mat) SRS) resulted in growth retardation (Shiura H et al 2009) whereas loss of *GRB10* results in fetal overgrowth (Abu-Amero, S et al 2010). Thus the findings of this study suggests that epimutations at loci such as *GRB10* may play a role in SRS.

Current research

Research in the field of SRS, has significantly increased in recent years, with attentions focused on the molecular basis for the syndrome and understanding idiopathic SRS. As previously mentioned several studies have also looked at methylation at other imprinted loci including Peg1/ MEST, PEG10, *IGF2*PO and DLK (Turner, CLS et al 2010; Peñaherrera, M. et al 2009; Azzi et al 2009). Findings within this field have shown that LOM at other imprinted loci are not as common as one might have first hypothesised, and do not appear to affect phenotype, leaving many questions still unanswered.

Other studies have investigated mutations in candidate genes as possible causes of SRS. Jager. S et al 2009 focused on mutations in *PLAGL1* while Eaggermann, T et al predominantly focused on *GNAS*. Neither study found any point mutation or copy number variable (CNV) that could be attributed to SRS. Other investigations have focused on looking for mutations, deletions or rearrangements around the *H19* locus. A preliminary study by Grønskov K et al 2011 of 4 patients with suspected SRS, identified breakpoints and disruptions of the shared *H19*/*IGF2* enhancer region, in all individuals. Demars, J et al 2011 also identified a novel duplication in part of *H19/IGF2* imprinting control, which resulted in a SRS phenotype only if maternally inherited when investigating SNPs within the 11q15 imprinted region in 72 SRS patients who displayed LOM at ICR1. While Adkins RM et al 2010, identified a SNP near the CTCF binding site, which has been associated with birth weight. These studies highlight the need to examine not only the enhancer and regulatory regions of imprinted genes but also promoter-enhancer interactions in individuals with imprinting defects.

Genome wide searches for SNPs and microdeletions have also been conducted to pinpoint candidate regions or genes associated with SRS. In the case of Lyn, SY et al 2010, a study on 34 SRS individuals highlighted five microdeletions in 14.7% of the population tested, though further investigation has yet to be carried out to determine any link with SRS.

In an attempt to further understand SRS, other groups have begun investigating the proteins involved in silencing gene expression via DNA methylation, such as methyl-CpG binding (MBD) proteins that preferentially bind to methylated DNA and facilitate recruitment of other transcription repressive proteins such as histone deacetylases. In mice reduced levels of MBD3 resulted in LOM at the ICR1 (*H19*), thus providing a candidate protein for SRS. However Bachmann et al 2009 have since identified that mutations in MBD3 are not responsible of the LOM at *H19* that is so frequently observed in SRS. Other groups have begun to investigate if the intrauterine environment attributes to SRS, reporting that hypomethylation at *H19* has been found in the placentas of pregnancies associated with fetal growth restriction (Banister, CE. Et al 2011; Koukoura, O. et a 2011).

Ongoing research highlights the complexity of SRS with many factors affecting the phenotype. Studies such as the current report are important to progress the understanding of this multifactorial syndrome. .

Limitations of this study

Investigation of methylation state at imprinted loci using BA biosciences EpiTect Methyl Profiler is a relatively novel technique, with this assay predominantly

being used for cancer methylation analysis. It claims to produce results comparable to bisulfite sequencing and permits the analysis of multiple samples or genes at one time and could have huge potential in semi high-throughput analysis of methylation states (SA Bioscience methylation flyer). http://www.sabiosciences.com/manuals/Methyl_FLYER_lo.pdf

Nevertheless the GOM or LOM results obtained in this study should be confirmed by a widely accepted method such as methylation specific PCR or bisulphate sequencing. One sample included in this study (SR18) had already had the methylation state of several loci previously tested via the above-mentioned techniques. The results of these investigations produced the same conclusions for this individual as using the EpiTect Methyl Profiler, indicating that this method is likely to be reliable and provide accurate results.

Another limitation with this study was the number of loci tested; *www.geneimprint.com* published a list of known and predicted imprinted loci in humans. Although the loci investigated here were selected for their potential involvement in SRS, many more have yet to be studied in relation to SRS.

Though a reasonable size cohort was used, larger studies have been conducted, allowing for the identification of rare events and allowing more accurate quantification, of any observation made.

The most common method for molecular diagnosis of SRS, is by examining lymphocyte DNA, therefore most DNA used in this study is derived from patients lymphocytes, however many reports have been conducted in both BWS and SRS

patients, highlighting the presence of imprinting mosaicism, (Peñaherrera, M. et al 2009) with differences in hypomethylation even being observed between different sides of the oral cavity in one individual (Begemann, M et al 2010). This phenomenon could potentially result in cases being misdiagnosed, and methylation abnormalities being missed.

Future directions

It is clear that we are still a long way off from determining the molecular causes behind SRS, and that much more research needs to be done; it is therefore proposed that future work should be focused on obtaining quantitive high throughput methylation profiles of CpG islands in SRS via techniques such as Illumina methylation assays, and within 5 years, the cost of whole genome bisulfite sequencing should be comparable to allow whole genome methylation analysis. Comparing methylation states of multiple loci, imprinted or not in long non coding regions of large cohorts of SRS patients (including *H19* LOM, UPD7 (mat) and idiopathic patients) to control populations (both normal gestational size, and small gestation age non-SRS individuals) novel epimutions and regulatory regions in non coding DNA may be identified. However this type of study is currently limited by economical constraints . In depth clinical data for all participants of future studies should also be acquired where possible allowing epigenotype/ phenotype comparisons. Analysis the methylation of several different tissues per individual, for example, leukocytes and buccal swab DNA should also be included in future studies.

In conclusion, this study identifies that aberrant methylation at loci other than *H19*, is more common in SRS suffers that already present with LOM at *H19*, although this observation is only present in 33% of *H19* SRS individuals.

References

ABU-AMERO, S., WAKELING, E. L., PREECE, M., WHITTAKER, J., STANIER, P. & MOORE, G. E. 2010. Epigenetic signatures of Silver-Russell syndrome. J Med Genet, 47, 150-4.

ADKINS, R. M., SOMES, G., MORRISON, J. C., HILL, J. B., WATSON, E. M., MAGANN, E. F. & KRUSHKAL, J. 2010. Association of birth weight with polymorphisms in the *IGF2*, *H19*, and *IGF2R* genes. Pediatr Res, 68, 429-34.

AZZI, S., ROSSIGNOL, S., STEUNOU, V., SAS, T., THIBAUD, N., DANTON, F., LE JULE, M., HEINRICHS, C., CABROL, S., GICQUEL, C., LE BOUC, Y. & NETCHINE, I. 2009. Multilocus methylation analysis in a large cohort of 11p15-related foetal growth disorders (Russell Silver and Beckwith Wiedemann syndromes) reveals simultaneous loss of methylation at paternal and maternal imprinted loci. Hum Mol Genet, 18, 4724-33.

BANISTER, C. E., KOESTLER, D. C., MACCANI, M. A., PADBURY, J. F., HOUSEMAN, E. A. & MARSIT, C. J. 2011. Infant growth restriction is associated with distinct patterns of DNA methylation in human placentas. Epigenetics, 6, 920-7.

BARTHOLDI, D., KRAJEWSKA-WALASEK, M., OUNAP, K., GASPAR, H., CHRZANOWSKA, K. H., ILYANA, H., KAYSERILI, H., LURIE, I. W., SCHINZEL, A. & BAUMER, A. 2009a. Epigenetic mutations of the imprinted *IGF2-H19* domain in Silver-Russell syndrome (SRS): results from a large cohort of patients with SRS and SRS-like phenotypes. J Med Genet, 46, 192-7.

BARTHOLDI, D., KRAJEWSKA-WALASEK, M., OUNAP, K., GASPAR, H., CHRZANOWSKA, K. H., ILYANA, H., KAYSERILI, H., LURIE, I. W., SCHINZEL, A. & BAUMER, A. 2009b. Epigenetic mutations of the imprinted *IGF2-H19* domain in Silver-Russell syndrome (SRS): results from a large cohort of patients with SRS and SRS-like phenotypes. J Med Genet, 46, 192-7.

BACHMANN, N., SPENGLER, S., BINDER, G. & EGGERMANN, T. 2010. MBD3 mutations are not responsible for ICR1 hypomethylation in Silver-Russell syndrome. Eur J Med Genet, 53, 23-4.

BEGEMANN, M., SPENGLER, S., KANBER, D., HAAKE, A., BAUDIS, M., LEISTEN, I., BINDER, G., MARKUS, S., RUPPRECHT, T., SEGERER, H., FRICKE-OTTO, S., M‹HLENBERG, R., SIEBERT, R., BUITING, K. & EGGERMANN, T. 2011. Silver-Russell patients showing a broad range of ICR1 and ICR2 hypomethylation in different tissues. Clin Genet, 80, 83-8.

BELL, A. C. & FELSENFELD, G. 2000. Methylation of a CTCF-dependent boundary controls imprinted expression of the *IGF2* gene. Nature, 405, 482-5.

BILL, B. R., PETZOLD, A. M., CLARK, K. J., SCHIMMENTI, L. A. & EKKER, S. C. 2009. A primer for morpholino use in zebrafish. Zebrafish, 6, 69-77.

BLIEK, J., VERDE, G., CALLAWAY, J., MAAS, S. M., DE CRESCENZO, A., SPARAGO, A., CERRATO, F., RUSSO, S., FERRAIUOLO, S., RINALDI, M. M., FISCHETTO, R., LALATTA, F., GIORDANO, L., FERRARI, P., CUBELLIS, M. V., LARIZZA, L., TEMPLE, I. K., MANNENS, M. M., MACKAY, D. J. & RICCIO, A. 2009a. Hypomethylation at

multiple maternally methylated imprinted regions including *PLAGL1* and *GNAS* loci in Beckwith-Wiedemann syndrome. Eur J Hum Genet, 17, 611-9.

BLIEK, J., VERDE, G., CALLAWAY, J., MAAS, S. M., DE CRESCENZO, A., SPARAGO, A., CERRATO, F., RUSSO, S., FERRAIUOLO, S., RINALDI, M. M., FISCHETTO, R., LALATTA, F., GIORDANO, L., FERRARI, P., CUBELLIS, M. V., LARIZZA, L., TEMPLE, I. K., MANNENS, M. M., MACKAY, D. J. & RICCIO, A. 2009. Hypomethylation at multiple maternally methylated imprinted regions including *PLAGL1* and *GNAS* loci in Beckwith-Wiedemann syndrome. Eur J Hum Genet, 17, 611-9.

BOWDIN, S., ALLEN, C., KIRBY, G., BRUETON, L., AFNAN, M., BARRATT, C., KIRKMAN-BROWN, J., HARRISON, R., MAHER, E. R. & REARDON, W. 2007. A survey of assisted reproductive technology births and imprinting disorders. Hum Reprod, 22, 3237-40.

BRAND, M., HEISENBERG, C. P., WARGA, R. M., PELEGRI, F., KARLSTROM, R. O., BEUCHLE, D., PICKER, A., JIANG, Y. J., FURUTANI-SEIKI, M., VAN EEDEN, F. J., GRANATO, M., HAFFTER, P., HAMMERSCHMIDT, M., KANE, D. A., KELSH, R. N., MULLINS, M. C., ODENTHAL, J. & N‹SSLEIN-VOLHARD, C. 1996. Mutations affecting development of the midline and general body shape during zebrafish embryogenesis. Development, 123, 129-42.

BRUCE, S., HANNULA-JOUPPI, K., PELTONEN, J., KERE, J. & LIPSANEN-NYMAN, M. 2009. Clinically distinct epigenetic subgroups in Silver-Russell syndrome: the degree of *H19* hypomethylation associates with phenotype severity and genital and skeletal anomalies. J Clin Endocrinol Metab, 94, 579-87.

BUTLER, M. G. 2009. Genomic imprinting disorders in humans: a mini-review. J Assist Reprod Genet, 26, 477-86.

CHANG, L. L. & KESSLER, D. S. 2010. Foxd3 is an essential Nodal-dependent regulator of zebrafish dorsal mesoderm development. Dev Biol, 342, 39-50.

CHARALAMBOUS, M., SMITH, F. M., BENNETT, W. R., CREW, T. E., MACKENZIE, F. & WARD, A. 2003. Disruption of the imprinted *GRB10* gene leads to disproportionate overgrowth by an *IGF2*-independent mechanism. Proc Natl Acad Sci U S A, 100, 8292-7.

Chen Lab protocols Stanford University: http://chen.stanford.edu/documents/DechorionationProtocol.pdf

DEMARS, J., ROSSIGNOL, S., NETCHINE, I., SYIN LEE, K., SHMELA, M., FAIVRE, L., WEILL, J., ODENT, S., AZZI, S., CALLIER, P., LUCAS, J., DUBOURG, C., ANDRIEUX, J., LE BOUC, Y., EL-OSTA, A. & GICQUEL, C. 2011. New insights into the pathogenesis of Beckwith-Wiedemann and Silver-Russell syndromes: Contribution of small copy number variations to 11p15 imprinting defects. Hum Mutat.

EGGERMANN, T. 2010. Russell-Silver syndrome. Am J Med Genet C Semin Med Genet, 154C, 355-64.

EGGERMANN, T., EGGERMANN, K. & SCH÷NHERR, N. 2008. Growth retardation versus overgrowth: Silver-Russell syndrome is genetically opposite to Beckwith-Wiedemann syndrome. Trends Genet, 24, 195-204.

EGGERMANN, T., MEYER, E., SCH÷NHERR, N., FLICK, F., CHAUVISTR…, H., MAVANY, M. & WOLLMANN, H. A. 2007. Mutation analysis of *GNAS*1 and overlapping transcripts in Silver-Russell syndrome patients. Mol Genet Metab, 90, 224-6.

EISEN, J. S. & SMITH, J. C. 2008. Controlling morpholino experiments: don't stop making antisense. Development, 135, 1735-43.

EPSTEIN, D. J. 2009. Cis-regulatory mutations in human disease. Brief Funct Genomic Proteomic, 8, 310-6.

FLEMING, A. 2006. Zebrafish as an alternative model organism for disease modeling and drug discovery: implications for the 3Rs. National centre for the Replacement, Refinement and Reduction of animals in research.

GEHRIG, J., REISCHL, M., KALMAR, E., FERG, M., HADZHIEV, Y., ZAUCKER, A., SONG, C., SCHINDLER, S., LIEBEL, U. & MULLER, F. 2009. Automated high-throughput mapping of promoter-enhancer interactions in zebrafish embryos. Nat Methods, 6, 911-6.

GERETY, S. S. & WILKINSON, D. G. 2011. Morpholino artifacts provide pitfalls and reveal a novel role for pro-apoptotic genes in hindbrain boundary development. Dev Biol, 350, 279-89.

GICQUEL, C., ROSSIGNOL, S., CABROL, S., HOUANG, M., STEUNOU, V., BARBU, V., DANTON, F., THIBAUD, N., LE MERRER, M., BURGLEN, L., BERTRAND, A. M., NETCHINE, I. & LE BOUC, Y. 2005. Epimutation of the telomeric imprinting

center region on chromosome 11p15 in Silver-Russell syndrome. Nat Genet, 37, 1003-7.

GRØNSKOV, K., POOLE, R. L., HAHNEMANN, J. M., THOMSON, J., TÜMER, Z., BRØNDUM-NIELSEN, K., MURPHY, R., RAVN, K., MELCHIOR, L., DEDIC, A., DOLMER, B., TEMPLE, I. K., BOONEN, S. E. & MACKAY, D. J. 2011. Deletions and rearrangements of the *H19*/*IGF2* enhancer region in patients with Silver-Russell syndrome and growth retardation. J Med Genet, 48, 308-11.

JÄGER, S., SCHÖNHERR, N., SPENGLER, S., RANKE, M. B., WOLLMANN, H. A., BINDER, G. & EGGERMANN, T. 2009. LOT1 (ZAC1/*PLAGL1*) as member of an imprinted gene network does not harbor Silver-Russell specific variants. J Pediatr Endocrinol Metab, 22, 555-9.

JOPLING, C., SLEEP, E., RAYA, M., MARTÕ, M., RAYA, A. & BELMONTE, J. C. 2010. Zebrafish heart regeneration occurs by cardiomyocyte dedifferentiation and proliferation. Nature, 464, 606-9.

KIMMEL, C. B., BALLARD, W. W., KIMMEL, S. R., ULLMANN, B. & SCHILLING, T. F. 1995. Stages of embryonic development of the zebrafish. Dev Dyn, 203, 253-310.

KINNA, G., KOLLE, G., CARTER, A., KEY, B., LIESCHKE, G. J., PERKINS, A. & LITTLE, M. H. 2006. Knockdown of zebrafish crim1 results in a bent tail phenotype with defects in somite and vascular development. Mech Dev, 123, 277-87.

KOUKOURA, O., SIFAKIS, S., ZARAVINOS, A., APOSTOLIDOU, S., JONES, A., HAJIIOANNOU, J., WIDSCHWENDTER, M. & SPANDIDOS, D. A. 2011.

Hypomethylation along with increased *H19* expression in placentas from pregnancies complicated with fetal growth restriction. Placenta, 32, 51-7.

KREBS, A. 2010 Functional characterization of GCN5 containing complexes. Doctoral thesis. University of Strasbourg.

KREBS, A. R., DEMMERS, J., KARMODIYA, K., CHANG, N. C., CHANG, A. C. & TORA, L. 2010. ATAC and Mediator coactivators form a stable complex and regulate a set of non-coding RNA genes. EMBO Rep, 11, 541-7.

KREBS, A.R. KARMODIYA, K. LINDAHL-ALLEN, M. STRUHL, K. & TORA, L. 2011. SAGA and ATAC histone acetyl transferase complexes regulate distinct sets of genes and ATAC-defines a new class of p300-independent enhancers. Submitted for publication January 2011.

LE BOUC, Y., ROSSIGNOL, S., AZZI, S., STEUNOU, V., NETCHINE, I. & GICQUEL, C. 2010. Epigenetics, genomic imprinting and assisted reproductive technology. Ann Endocrinol (Paris), 71, 237-8.

Lim, D HK; and Maher, R. 2009. Human imprinting syndromes. Epigenomics, Volume 1, Number 2, pp. 347-369(23)

LIM, D. H. & MAHER, E. R. 2010. Genomic imprinting syndromes and cancer. Adv Genet, 70, 145-75.

LIM, D., BOWDIN, S. C., TEE, L., KIRBY, G. A., BLAIR, E., FRYER, A., LAM, W., OLEY, C., COLE, T., BRUETON, L. A., REIK, W., MACDONALD, F. & MAHER, E. R. 2009.

Clinical and molecular genetic features of Beckwith-Wiedemann syndrome associated with assisted reproductive technologies. Hum Reprod, 24, 741-7.

LIN, S. Y., LEE, C. N., HUNG, C. C., TSAI, W. Y., LIN, S. P., LI, N. C., HSIEH, W. S., TUNG, Y. C., NIU, D. M., HSU, W. M., CHEN, L. Y., FANG, M. Y., TU, M. P., KUO, P. W., LIN, C. Y., SU, Y. N. & HO, H. N. 2010. Epigenetic profiling of the *H19* differentially methylated region and comprehensive whole genome array-based analysis in Silver-Russell syndrome. Am J Med Genet A, 152A, 2521-8.

MCGRAW, H. F., NECHIPORUK, A. & RAIBLE, D. W. 2008. Zebrafish dorsal root ganglia neural precursor cells adopt a glial fate in the absence of neurogenin1. J Neurosci, 28, 12558-69.

NAGY, Z., RISS, A., FUJIYAMA, S., KREBS, A., ORPINELL, M., JANSEN, P., COHEN, A., STUNNENBERG, H. G., KATO, S. & TORA, L. 2010. The metazoan ATAC and SAGA coactivator HAT complexes regulate different sets of inducible target genes. Cell Mol Life Sci, 67, 611-28.

NOLIS, I. K., MCKAY, D. J., MANTOUVALOU, E., LOMVARDAS, S., MERIKA, M. & THANOS, D. 2009. Transcription factors mediate long-range enhancer-promoter interactions. Proc Natl Acad Sci U S A, 106, 20222-7.

OHLSSON, R., BARTKUHN, M. & RENKAWITZ, R. 2010. CTCF shapes chromatin by multiple mechanisms: the impact of 20 years of CTCF research on understanding the workings of chromatin. Chromosoma, 119, 351-60.

ORPINELL, M., FOURNIER, M., RISS, A., NAGY, Z., KREBS, A. R., FRONTINI, M. & TORA, L. 2010. The ATAC acetyl transferase complex controls mitotic progression by targeting non-histone substrates. EMBO J, 29, 2381-94.

OWEN, C. M. & SEGARS, J. H. 2009. Imprinting disorders and assisted reproductive technology. Semin Reprod Med, 27, 417-28.

PEÑAHERRERA, M. S., WEINDLER, S., VAN ALLEN, M. I., YONG, S. L., METZGER, D. L., MCGILLIVRAY, B., BOERKOEL, C., LANGLOIS, S. & ROBINSON, W. P. 2010. Methylation profiling in individuals with Russell-Silver syndrome. Am J Med Genet A, 152A, 347-55.

PHILLIPS, B. T., KWON, H. J., MELTON, C., HOUGHTALING, P., FRITZ, A. & RILEY, B. B. 2006. Zebrafish msxB, msxC and msxE function together to refine the neural-nonneural border and regulate cranial placodes and neural crest development. Dev Biol, 294, 376-90.

SA Bioscience methylation flyer
http://www.sabiosciences.com/manuals/Methyl_FLYER_lo.pdf

SA biosciences EpiTect Methyl qPCR assay Manuel
http://www.sabiosciences.com/support_manual.php?pfamily=dnamethylation).

SCHÖNHERR, N., MEYER, E., BINDER, G., WOLLMANN, H. A. & EGGERMANN, T. 2007. No evidence for additional imprinting defects in Silver-Russell syndrome patients with maternal uniparental disomy 7 or 11p15 epimutation. J Pediatr Endocrinol Metab, 20, 1329-31.

SHIURA, H., NAKAMURA, K., HIKICHI, T., HINO, T., ODA, K., SUZUKI-MIGISHIMA, R., KOHDA, T., KANEKO-ISHINO, T. & ISHINO, F. 2009. Paternal deletion of Meg1/*GRB10* DMR causes maternalization of the Meg1/*GRB10* cluster in mouse proximal Chromosome 11 leading to severe pre- and postnatal growth retardation. Hum Mol Genet, 18, 1424-38.

SUGANUMA, T., MUSHEGIAN, A., SWANSON, S. K., ABMAYR, S. M., FLORENS, L., WASHBURN, M. P. & WORKMAN, J. L. 2010. The ATAC acetyltransferase complex coordinates MAP kinases to regulate JNK target genes. Cell, 142, 726-36.

TAMURA, T., TOHMA, T., OHTA, T., SOEJIMA, H., HARADA, N., ABE, K. & NIIKAWA, N. 1993. Ring chromosome 15 involving deletion of the insulin-like growth factor 1 receptor gene in a patient with features of Silver-Russell syndrome. Clin Dysmorphol, 2, 106-13.

TURNER, C. L., MACKAY, D. M., CALLAWAY, J. L., DOCHERTY, L. E., POOLE, R. L., BULLMAN, H., LEVER, M., CASTLE, B. M., KIVUVA, E. C., TURNPENNY, P. D., MEHTA, S. G., MANSOUR, S., WAKELING, E. L., MATHEW, V., MADDEN, J., DAVIES, J. H. & TEMPLE, I. K. 2010. Methylation analysis of 79 patients with growth restriction reveals novel patterns of methylation change at imprinted loci. Eur J Hum Genet, 18, 648-55.

UCSC; http://genome.ucsc.edu/ Zebrafish genome v9

WAKELING, E. L., AMERO, S. A., ALDERS, M., BLIEK, J., FORSYTHE, E., KUMAR, S., LIM, D. H., MACDONALD, F., MACKAY, D. J., MAHER, E. R., MOORE, G. E., POOLE, R. L., PRICE, S. M., TANGERAAS, T., TURNER, C. L., VAN HAELST, M. M.,

WILLOUGHBY, C., TEMPLE, I. K. & COBBEN, J. M. 2010. Epigenotype-phenotype correlations in Silver-Russell syndrome. J Med Genet, 47, 760-8.

WANG, Y. L., FAIOLA, F., XU, M., PAN, S. & MARTINEZ, E. 2008. Human ATAC Is a GCN5/PCAF-containing acetylase complex with a novel NC2-like histone fold module that interacts with the TATA-binding protein. J Biol Chem, 283, 33808-15.

WESTERFIELD, M. The Zebrafish book. (University of Oregon Press, Eugene, Oregon, USA, 1995).

WILSON, G. N., SAUDER, S. E., BUSH, M. & BEITINS, I. Z. 1985. Phenotypic delineation of ring chromosome 15 and Russell-Silver syndromes. J Med Genet, 22, 233-6.

YOSHIHASHI, H., MAEYAMA, K., KOSAKI, R., OGATA, T., TSUKAHARA, M., GOTO, Y., HATA, J., MATSUO, N., SMITH, R. J. & KOSAKI, K. 2000. Imprinting of human *GRB10* and its mutations in two patients with Russell-Silver syndrome. Am J Hum Genet, 67, 476-82.

Zfin.org neurogenin 1;http://zfin.org/cgi-bin/webdriver?MIval=aa-markerview.apg&OID=ZDB-GENE-990415-174

Appendix 1: Clinical data for individual SRS cases

Case	*H19* methylation state	Contception and gestation	Perinatal period <1 month	Postnatal Period >1 month	Other clinical clinical features
SR01	LOM	Normal conception; 32 week gestation	Required intensive care	No Feeding difficulties reported	Right arm and leg hemihypertrophy, prominent forehead, down turned mouth
SR02	LOM	Normal conception; 38 week gestation	No reported problems	Feeding difficulties	Right leg hemihypertrophy, facial asymmetry, prominent forehead, micrognathia and fifth finger clinodactyly
SR03	LOM	Normal conception; 40 week gestation	Required intensive care	No Feeding difficulties reported, small café au lait patches	Mild facial asymmetry, down turned mouth, fifth finger clinodactyly ,short rightfifth finger, mild left ptosis and anteverted ears.
SR04	LOM	ART; 39 weeks gestation	Feeding difficulties, Tube feed	No Feeding difficulties reported	Face, arm , leg and trunk hemihypertrophy, facial asymmetry and prominent forehead.
SR05	LOM	Normal conception; 37 week gestation	Required intensive care, No feeding difficulties	Gastro reflux	Right leg hemihypertrophy, facial asymmetry, prominent forehead, mild micrognathia and fifth finger clinodactyly
SR06	LOM	Normal conception; 36 week gestation	Required intensive care, with feeding difficulties	Feeding difficulties	Prominent forhead, down turned mouth fifth finger clinodactyly and stork mark on nape of neck
SR07	LOM	Normal conception; 38 week gestation	Required intensive care, with Feeding difficulties and Hypoglycaemia	Feeding difficulties	Left hemihypertrophy, mild facial asymmetry, prominent forehead and dental crowding
SR08	LOM	Normal conception; 38 week gestation	No reported problems	No Feeding difficulties reported	Left leg hemihypertrophy, prominent forehead and fifth finger clinodactyly
SR09	LOM	Normal conception; 34 week gestation	Feeding difficulties and Hypoglycemia	Feeding difficulties; nasogastric tube fed and Gastrostomy; Mental retadation	Hemihypertrophy, prominent forehead, down turned mouth, fifth finger clinodactyly and camptodactyly

SR10	LOM	Normal conception; 37 week gestation	Required intensive care,with feeding difficulties and Hypoglycaemia	Feeding difficulties	Delayed bone age, facial asymmetry, prominent forehead, down turned mouth, micrognathia, fifth finger clinodactyly and Patent ductus arteriosus (PDA)
SR11	LOM	Normal conception; 34 week gestation	Required intensive care	No Feeding difficulties reported	Mild delayed bone age, prominent forehead, down turned mouth, micrognathia and fifth finger clinodactyly
SR12	LOM	Normal conception; 40 week gestation	No reported problems	Feeding difficulties	Facial asymmetry, prominent forehead, down turned mouthand fifth finger clinodactyly
SR13	LOM	ICSI; 27 weeks gestation	Required intensive care, with feeding difficulties	Feeding difficulties; visual defects and mental retardation	Leg hemihypertrophy, delayed bone age, prominent forehead, down turned mouth, fifth fingure clinodactyly, slight deepset eyes and trivial PDA
SR14	LOM	Normal conception; 40 week gestation	No reported problems	Unknown	Prominent forhead, down turned mouth, fifth finger clinodactyly and camptodactyly
SR15	LOM	Normal conception; 40 week gestation	Required intensive care, with feeding difficulties	Feeding difficulties; Nasogastric tube fed; Mental retardation	Right side hemihypertrophy, prominent forehead, down turned mouth, micrognathia, fifth finger clinodactyly
SR16	LOM	Normal conception; 40 week gestation	Feedng difficulties	Feeding difficulties	Leg hemihypertrophy, prominent forehead, down turned mouth, fifth fingure clinodactyly.
SR17	LOM	Normal conception; 39 week gestation	Required intensive care, with feeding difficulties and Hypoglycaemia	Feeding difficulties	Left arm and leg hemihypertrophy, prominent forehead and fifth finger clinodactyly
SR18	LOM	ICSI conception	At 2yr 3 months; typical BWS phenotype with overgrowth (postnatal onset), macroglossia, abnormal umbilicus, ear lobe creases and asymmetry and other features. Fits criteria for BWS clinical diagnosis. **Other atypical features**; unsteady gait and facial phenotype (simular to AS/PWS) **Molecular info**: *SNRPN* methylation normal LOM *H19 PLAGL1* and MEST		
SR19	Normal	ART; 37 week gestation	Feedng difficulties	Feeding difficulties	Delayed bone age
SR20	Normal	Normal conception; 38 weeks gestation	No reported problems	No Feeding difficulties reported	Facial asymmetry and prominent forehead

SR21	Normal	40 weeks gestation	Feedng difficulties	Feeding difficulties	None reported
SR22	Normal	Normal conception; 28 week gestation	Required intensive care, No feeding difficulties	No Feeding difficulties reported	Elfin features
SR23	Normal	Normal conception; 40 week gestation	Feedng difficulties	Feeding difficulties	left arm hemihypertrophy, prominent forehead, down turned mouth congenital cardiac malformations and low set ear on Right
SR24	Normal	Normal conception; 33 week gestation	Required intensive care,with feeding difficulties	No Feeding difficulties reported; but nasogastric tube fed	Flat philtrum, full cheeks and congenital cardiac malformations
SR25	Normal	Normal conception; 38 week gestation	No reported problems	Feeding difficulties; Mental retardation	Triangular face, hemihypertrophy, prominent forehead, down turned mouth and fifth finger clinodactyly
SR26	Normal	Normal conception; 40 week gestation	No reported problems	No Feeding difficulties reported; Mental retardation	right thorax and left leg hemihypertrophy, facial asymmetry, down turned mouth, fifth finger clinodactyly, short broad neck and congenital cardiac malformations
SR27	Normal	Normal conception; 28 week gestation	No reported problems	Feeding difficulties; nasogastric tube fed; Visual defects and Mental retardation	Unknown
SR28	Normal	Normal conception; 39 week gestation	Feedng difficulties	Feeding difficulties	Delayed bone growth, prominent forehead,up turned Nose, frontal cowslick to hair and gingiva.
SR29	Normal	Normal conception; 30 week gestation	Required intensive care, No feeding difficulties	Feeding difficulties; nasogastric tube fed, café au lait patches	Congenital cardiac malformation
SR30	Normal	Normal conception; 37 week gestation	Required intensive care, No feeding difficulties	Feeding difficultiesand Mental retardation	Mild face hypoplasia, small upturned nose, thin lip
SR31	Normal	Normal conception; 40 week gestation	Feeding difficulties and Hypoglycemia	Feeding difficulties	Prominent forehead, abnormal crease left palm

SR32	Normal	40 week gestation	Feeding difficulties and Hypoglycemia	Feeding difficulties; Visual defects and Mental retardation	Delayed bone age and fifth finger clinodactyly
SR33	Normal	Normal conception; 40 week gestation	No reported problems	No Feeding difficulties reported; Mild mental retardation; café au lait patches	Delayed bone age
SR34	Normal	Normal conception; 36 week gestation	Required intensive care, No feeding difficulties	No Feeding difficulties reported,café au lait patches	Prominent forehead and ears and triangular face
SR35	Normal	Normal conception; 39 week gestation	Feedng difficulties	Feeding difficulties; nasogastric tube fed and gastrostomy	Low set ears and fifth finger clinodactyly
SR36	Normal	Normal conception; 37 week gestation	No reported problems	No Feeding difficulties reported, café au lait patches	Facial asymmetry, prominent forehead, down turned mouth and fifth finger clinodactyly
SR37	Normal	Normal conception; 38 week gestation	Required intensive care, with feeding difficulties	Feeding difficulties	Right leg hermihypertrophy, prominent forehead and fifth finger clinodactyly
SR38	Normal	Normal conception; 38 week gestation	No reported problems	No Feeding difficulties reported; but nasogastric tube fed	Prominent forehead and down turned mouth
SR39	Normal	Normal conception; 38 week gestation	Feedng difficulties	Feeding difficulties	left hand and leg hemihypertrophy, delayed bone age, prominent forehead and fifth finger clinodactyly
SR40	Normal	ART; 31 weeks gestation	Required intensive care, No feeding difficulties	Feeding difficulties	Right leg hermihypertrophy, prominent forehead and fifth finger clinodactyly

UNIVERSITY OF
BIRMINGHAM

University of Birmingham Research Archive

e-theses repository

This unpublished thesis/dissertation is copyright of the author and/or third parties. The intellectual property rights of the author or third parties in respect of this work are as defined by The Copyright Designs and Patents Act 1988 or as modified by any successor legislation.

Any use made of information contained in this thesis/dissertation must be in accordance with that legislation and must be properly acknowledged. Further distribution or reproduction in any format is prohibited without the permission of the copyright holder.